28. CRETACEOUS VOLCANOGENIC SEDIMENTS FROM THE LINE ISLAND CHAIN: DIAGENESIS AND FORMATION OF K-FELDSPAR, DSDP LEG 33, HOLE 315A AND SITE 316

Kerry Kelts and Judith Anne McKenzie, Geological Institute ETH,
Swiss Federal Institute of Technology, Zurich, Switzerland

ABSTRACT

Upper Cretaceous volcanogenic sediments cored from the archipelagic aprons of the Line Islands chain (Hole 315A and Site 316) consist primarily of redeposited material comprised of altered volcanic glass, feldspars, mafic minerals, clays, and other products of alteration. Well-developed current structures and hyaloclastic textures are common. The sediments were apparently deposited rapidly as a sequence of turbidite-like beds interrupted by a few interludes of unknown duration. The most prominent interlude is marked by a zone of brightly variegated argillaceous material.

Bulk chemical analyses of the volcanogenic sediments revealed that they are relatively enriched in K, Fe, and Ti and depleted in Na, Ca, Al, and Si with respect to the source basalts. Mineralogically, this chemical discrepancy is reflected in the occurrence of compositionally pure K-feldspar (intermediate microcline) and potassium-rich clays in the volcanic sediments, particularly in the basal 50 meters (Campanian-Santonian). The K-feldspar appears to have a diagenetic origin resulting from early metasomatic replacement by low-temperature, potassium-enriched solutions. The replacement phenomena possibly reflect volcanic activity along the island chain. The inhomogeneous distribution of the K-feldspars in the sediments may represent transport of the solutions along graded beds that acted as conduits. A very slow diagenetic process has begun to alter the surface of the very stable, compositionally pure K-feldspars. This early breakdown is represented by three conspicuous stages of dissolution and phyllosilicate development.

In general, the clay mineral spectrum has a complex heterogeneous nature. The clay mixture contains pure montmorillonite phases, mixed-layer clays (illite/montmorillonite), and traces of illite (celadonite) and chlorite. Microscopic examination of the clays shows evidence that some were formed in situ and are an alteration product of the original detrital volcanic material. The mixed nature of the clay assemblage may result from a combination of early halmyrolysis of the volcanic clasts before significant burial, and progressive diagenesis throughout the sedimentary column.

Volcanogenic sedimentary sequences as encountered in Hole 315A and Site 316 appear to be widespread in the upper Cretaceous sediments from island chains in the Pacific and may indicate a simultaneous stratigraphic development.

INTRODUCTION

During Leg 33, thick sequences of Cretaceous, volcanogenic sediments were recovered from the basal sections at Hole 315A and Site 316 located on the archipelagic aprons of the Line Islands chain. In this chapter a detailed study of these sediments is reported. Primary emphasis is placed on the petrologic aspects of the investigated sections, especially on K-feldspar. These initial studies were broadened to cover the extent and type of diagenetic alteration in these sediments.

Volcanogenic, as used in this paper, is a term describing sediments that are derived from volcanic material. Volcanogenic sediments are produced by the transport of volcaniclastic material to the site of deposition and the in situ alteration of volcanic glass and minerals.

Little is known about average marine volcanogenic sediments, their weathering in a submarine environment (halmyrolysis), and their alteration after burial. Several recent petrologic studies (Hart, 1970; Moore, 1966; and Melson and Thompson, 1973) have indicated that during submarine weathering an exchange process is in operation which tends to give the samples a more alkali composition than the original basalt. Potassium enrichment is particularly significant. The rocks studied by these authors were in general quite recent, being fairly young basalts or dredged volcanogenic sediments.

There has been controversy over the importance of burial depth (pressure) versus temperature versus age as factors in diagenesis and the contribution of these and other factors to diagenesis. Because the volcanic sediments studied by us are of Late Cretaceous age, it was

hoped that information on the influence of depth of burial (P) and temperature (T) and age of diagenetic alterations could be gained.

Prior to the Deep Sea Drilling Project, the sampling of sections of volcanogenic sediments buried deep beneath the ocean floor had not been possible. In particular, Legs 15, 17, 19, and 32 changed this situation, and volcanogenic sediments as old as Late Cretaceous were secured from island chains. Previous to Leg 33, Leg 17, Hole 165A recovered Upper Cretaceous, volcanogenic sediments from the mid-Pacific archipelagic apron of the Line Islands (Winterer, Ewing, et al., 1973). We now had the opportunity to compare samples of the same age but from different depths in a sedimentary column and to compare samples of different ages.

The sediments we chose to study were derived from a presumably alkaline complex (Jackson et al., this volume) and allowed us to compare the nature or extent of alteration of these sediments with the underlying basement. Previous studies had treated the bulk composition of basaltic samples with emphasis on the breakdown of volcanic glass, the production of montmorillonite from mafic minerals, or the chemical balance. Our study emphasized the potassium-bearing phases in the sediments. During our initial, cursory examination of some sandy layers within the volcaniclastic sequences, we found concentrations of compositionally pure K-feldspar that appeared to be a replacement product. What was the origin of this K-feldspar?

With this question in mind, our continued, more extensive study placed special emphasis on these feldspars and their morphological development. Providing that the K-feldspars were early diagenetic products and compositionally pure end members, the examination of the slow alteration and surficial breakdown of a very stable phase in a low-temperature environment was possible. We also investigated some aspects of the clay mineralogy.

A variety of methods was utilized to study the material contained in the volcanogenic sediments. These included X-ray diffraction, microprobe, scanning electron microscopy with EDAX, X-ray fluorescence, and optical microscopy. Time considerations have limited the extent of this study.

GEOLOGIC SETTING AND STRATIGRAPHY

Hole 315A and Site 316 are located, respectively, in the vicinity of the present-day emergent Fanning and Christmas islands. These are part of the almost 3000-km-long Line Islands Seamount chain of volcanic edifices. Figure 1 shows the position of 315A and 316 as well as DSDP Sites 165A and 313 from which similar Upper Cretaceous lithologic sequences have been recovered (Winterer, Ewing, et al., 1973; Larson, Moberly, et al., 1974). Hole 315A and Site 316 were drilled 1035 and 867 meters, respectively, into the archipelagic apron of the Line Islands chain beginning in water depths of 4152 and 4451 meters, respectively.

A stratigraphic comparison of the Line Islands DSDP sites is presented in Figure 2 with the Cretaceous-Tertiary boundary as a datum plane. In summary, for the later discussion of depth-dependent alterations, note that Hole 315A contains about 150 meters of Upper Cretaceous volcanic sediment under 800 meters of overburden (Cores 21 to 30); Site 316 has at least 250 meters of volcanogenic sediment under 650 meters of overburden (Cores 19 to 30); whereas Hole 165A contains about 200 meters of volcanogenic sediment under only 300 meters of overburden. These sites yielded cores containing a variety of volcanogenic material, mostly as redeposited sediment. The overall amount of volcanic contribution is low in the Tertiary sediments, but generally increases downhole culminating in thick Campanian and Santonian (?) volcaniclastic sequences overlying a basaltic basement only reached in Hole 315A.

In the uppermost 800 meters of Hole 315A and Site 316 the contribution of volcanogenic material is limited to scattered volcanic grains and thin layers with palagonite, rare pyroxenes, feldspars, and glassy glomeroporphyritic clots. Commonly, they are concentrated in the basal part of graded foraminiferal grainstones. Some of the sand-sized grains include applotaxic clots, chlorite microlite grains, and rare altered feldspars. The presence of rare shallow-water benthonic foram assemblages (Beckmann, this volume), including Cretaceous forms, suggests that the volcanogenic sediments were derived from the submerged outer slopes of nearby seamounts. Cores 315A-24 to 30 and 316-19 to 30 recovered a complex section of graded and laminated volcanogenic sandstones, siltstones, and claystones interlayered with clayey limestones.

Cores 315A-27 to 30 and 316-22 to 28 often show a hyaloclastic texture in thin section (Plate 8). Some grains are rounded but most are highly angular. Volcaniclastic sedimentary beds commonly range from 1 cm up to 30 or 40 cm thick. They are mostly graded with the pelitic tops displaying a downward "exponential" burrowing. Within the body a variety of current structures are commonly visible. These include planar laminations, micrograding, cross-beds, scouring, flame structures, and rare signs of incipient sediment failure or convolute bedding. Hyaloclastic breccias were encountered in both Site 316 and Hole 165A (Winterer, Ewing, et al., 1973). However, they are absent in Hole 315A. This implies that Hole 315A may have been farther away from the presumed sediment supplying seamount.

Overall the color of the volcanogenic sediments ranges from light greenish-gray to dark greenish-black. Fine-grained claystones exhibit a light bluish-green color and waxy luster typical of montmorillonite clays. Interspersed are a few layers of light brown and white speckled sands. In Hole 315A Core 28, Section 3 and Core 29, Section 1 recovered a brightly colored series of blue, blue-green, and red interlayers. A thin limestone bed and a chert nodule were also encountered. Bright blue colorations appear to outline fluid motion along permeable sandstone layers and suggest that there has been significant in situ alteration)at these sites. The reader is referred to the special chapter on iron-titanium-rich basal sediments (Jenkyns and Hardy, this volume).

Most beds are stiff but friable. Cores in the volcanogenic series were conspicuous by the recovery of long unbroken plugs up to 120 cm and an even rate of drilling. The dominant cement is intergranular clay. In general, calcite cements are rare in the basal parts of

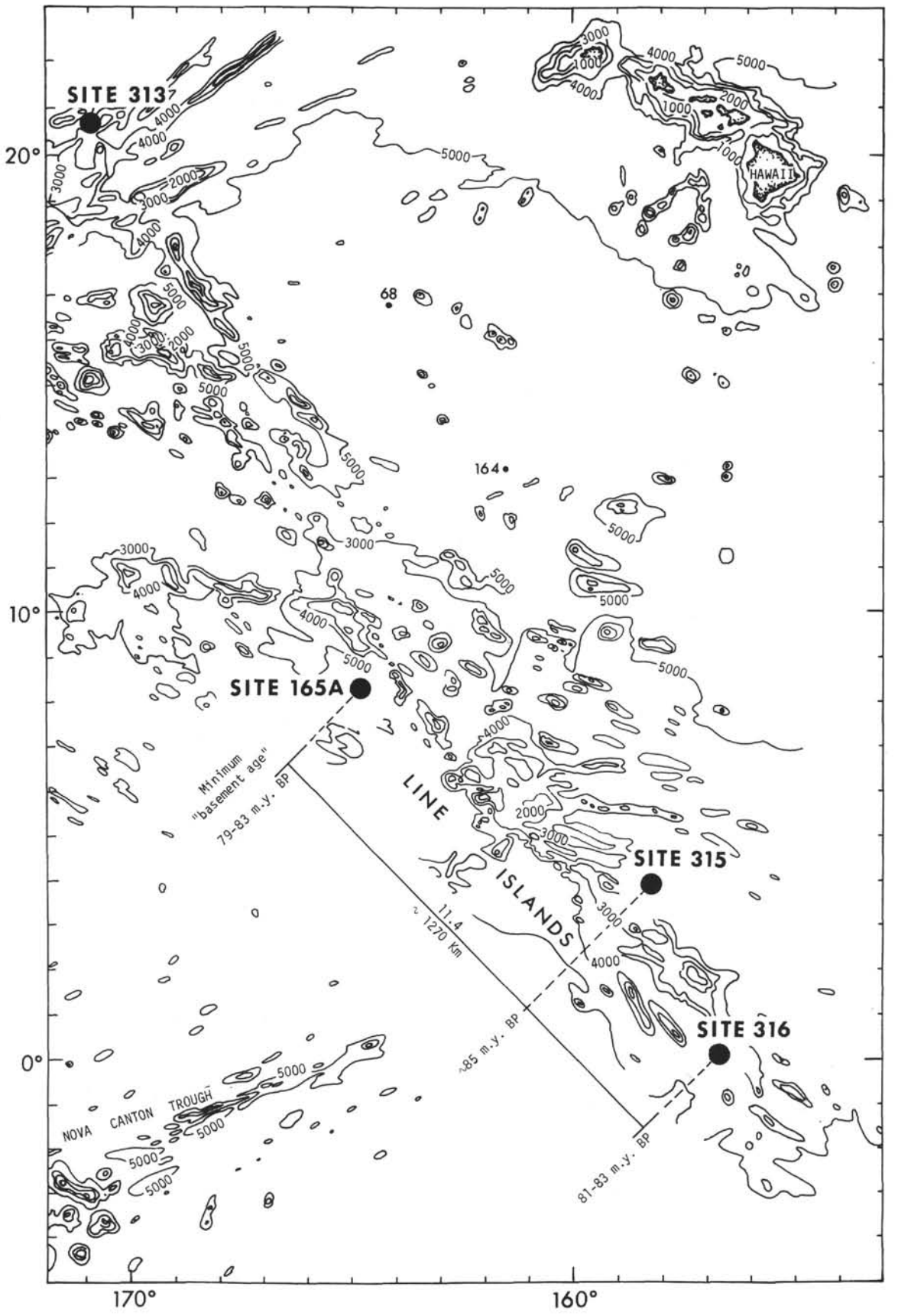

Figure 1. *Map showing the location of DSDP Leg 33 Hole 315 and Site 316 as well as Hole 165A and Site 313.*

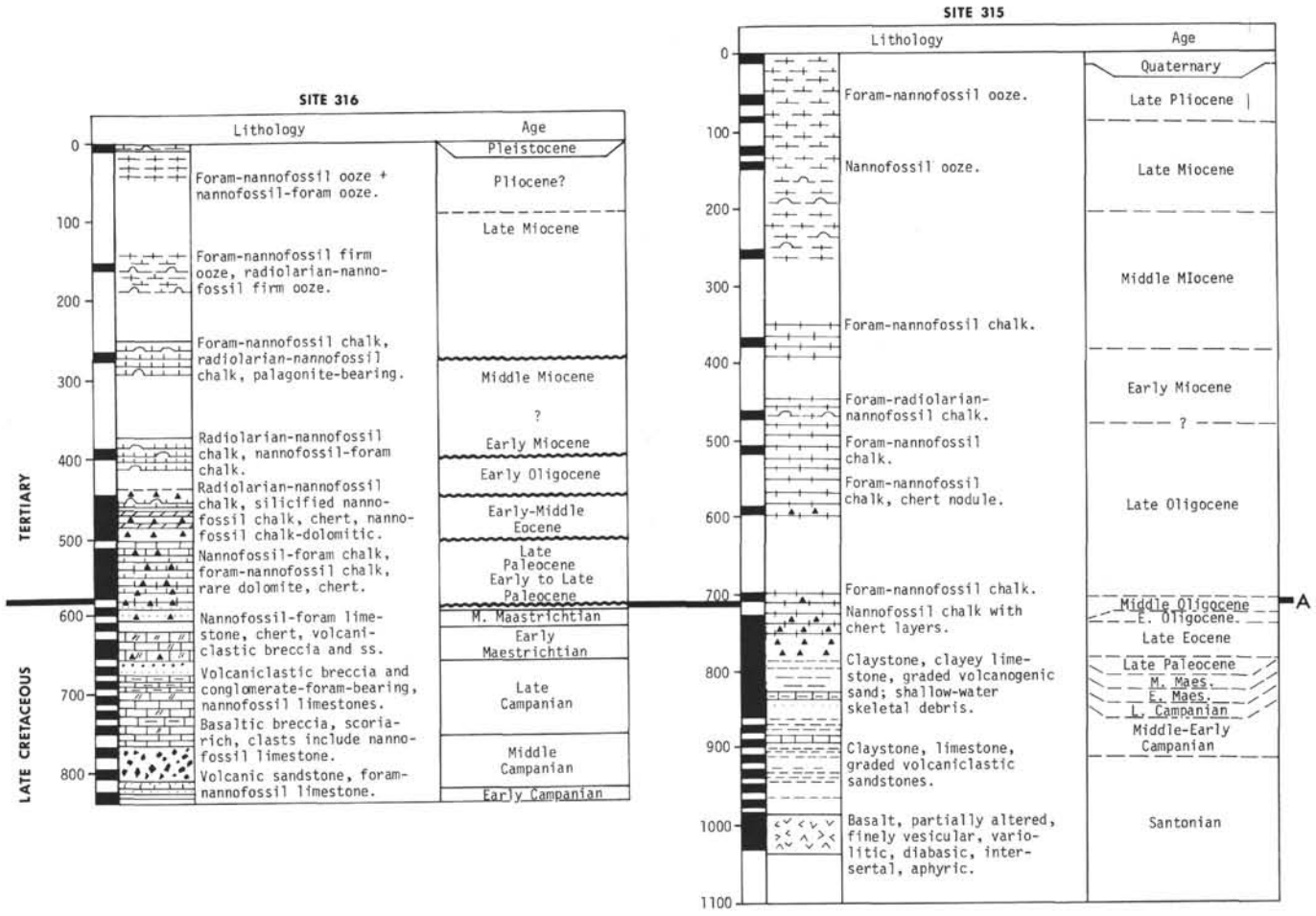

Figure 2. *Comparison of stratigraphy of Leg 33 Hole 315A and Site 316 with Hole 165A and Site 313. Note the differences in overburden of the Upper Cretaceous volcanogenic sediments.*

Hole 315A. Calcite cements or components were absent from Cores 315A-25 to 30. Calcite was even rare in vesicles in clasts of basaltic glass. An exception is in the zone of brightly colored interlayers. In contrast sparry calcite cement and calcareous components are a dominant feature of the volcanogenic sediments in the lower cores (19 to 30) of Site 316.

SOURCE AND SEDIMENTATION RATES

The primary sedimentary structures and component paragenesis of the volcanogenic sediments indicate that they have mostly been transported by currents. However, the abundance of irregular and subangular volcanic clasts implies that the distances of transport may not have been great. See Plates 1, 2, and 8 for thin-section micrographs illustrating these sediments. A rarity of fossils and calcareous material in the lowermost 100 meters of Hole 315A suggests that this sequence of turbidites was deposited simultaneously with or shortly after the last volcanic activity at this site. Graded volcanic sediment beds were formed as pyroclastic or hyaloclastic deposits were propelled in turbidity current fashion down the flanks of an eruption center.

The rates of sedimentation for such volcanogenic deposits is probably rapid and irregular, perhaps on the order of 100 m/m.y. However, the red and green interlayers from Section 315A-28-3 containing a few overgrown radiolarians imply that there were intermittent times of quiescence with sedimentation rates perhaps more on the order of 1 cm/m.y. The extent of the time lapse during the deposition of these sediments is difficult to estimate, but may represent several million years. Thus, the 85 m.y. basement age from Hole 315A may be considered a minimum age although not likely to be much older.

BASEMENT ROCKS

Basaltic flow units underlying the volcanogenic section from Hole 315A are described and discussed by Jackson et al. (this volume). A few aspects are summarized here pertinent to the understanding of the alteration products found in the overlying volcanic sediments. The basalts are interpreted to be mildly alkalic, similar in petrographic character to the alkaline volcanic rocks recovered from DSDP Hole 165A and to some basalts in the Hawaiian Islands (Bass et al., 1973). This is not inconsistent with the mineral and chemical composition of the overlying volcanic sediments. Jackson et al. (this volume) report that although flow textures are very well preserved, chemical alteration of the basalts is moderate to strong. A few fresh-looking plagioclases are present accompanied by rare scattered

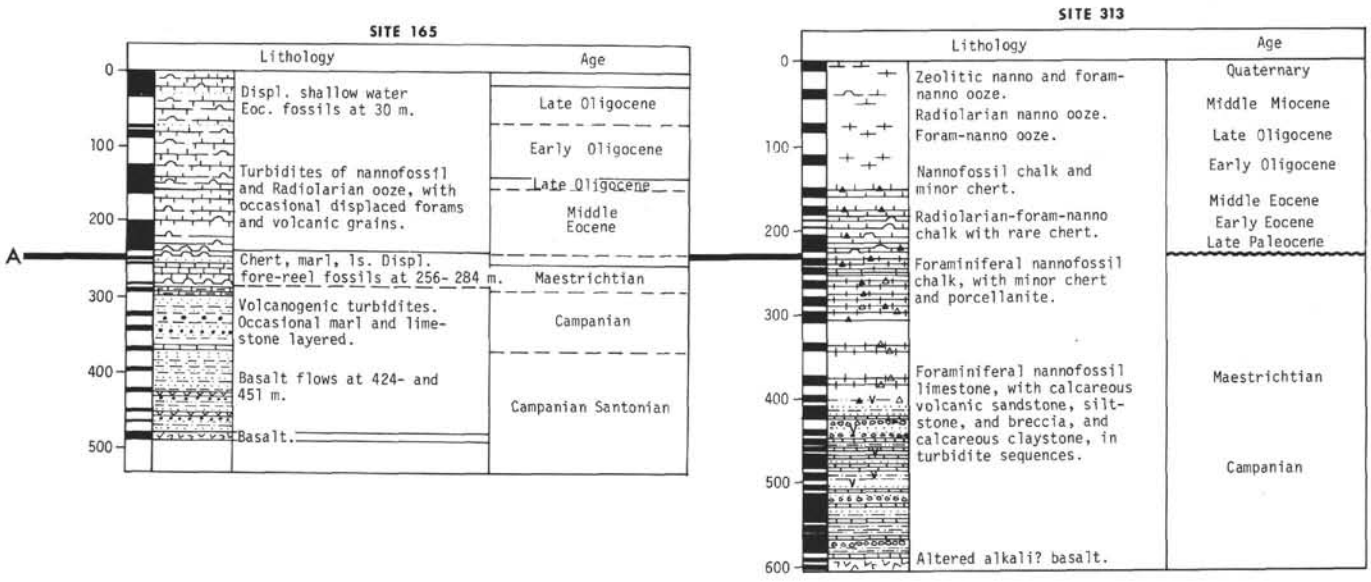

Figure 2. *(Continued).*

clinopyroxenes, but most glass and mafic components have been altered to montmorillonite minerals. Many vesicles are filled, some with calcite, others have a montmorillonite lining. In contrast to the overlying sediment, no K-feldspars were detected in any of the basalt flows. Other diagenetic minerals such as zeolites are rare. Jackson attributes most of the alteration to in situ breakdown.

The exact depths of Hole 315A and Site 316 at the time of deposition of the volcanic sediments during the Campanian and Santonian times are difficult to establish. Jackson et al. (this volume), however, report that the vesicle sizes seen in the basalt flows from Hole 315A are consistent with an emplacement below 2600 meters ruling out subareal weathering. A few radiolarians identified from interlayers in volcanogenic sediments from Hole 315A also point to a deep-water environment.

MINERALOGY

The Cretaceous volcanogenic sediments encountered in Hole 315A and Site 316 represent a wide spectrum of mineralogies. Trends are partly masked due to the sampling prejudices which tend to favor conspicuously unusual layers. Thin section descriptions and illustrations of textures, cements, and grain shapes are partly summarized in Plates 1 to 5. Routine, shore-based X-ray diffraction results reported by Cook and Zemmels (this volume) give some indication of the extent of alteration of the volcanic clasts.

We noted some of the following trends in X-ray results for samples of Upper Cretaceous sediments in Hole 315A, from about 830 meters to basement at 996 meters: K-feldspars are common, generally concentrated in the basal portions of greenish-gray, graded volcanic sands. They also occur in brownish layers. Montmorillonite is a dominant component of all the volcanic sands. Quartz is not commonly associated with K-feldspar-bearing layers, but can be a dominant constituent of some red and green claystone layers in association with mica minerals. It is also the major constituent of the black chert nodule from Core 28, Section 3. Calcite is a sporadic constituent, dominant above, but practically absent below Core 25. An exception was a bright blue-green limestone recorded from Sample 315A-28-3, 85 cm containing 93% calcite plus traces of montmorillonite, mica, hematite, and quartz. Aragonite, associated with quartz and mica, was reported from a thin creamy white layer from 315A-29-2, 85 cm. Zeolites are rare; only a significant component (clinoptilolite) in a light brown claystone (315A-27-2, 119 cm). Plagioclase is a consistent although mostly minor accessory mineral. Pyroxenes or amphiboles were not reported, but their recognition in a mixture is unlikely.

The red siltstone directly overlying the basement contained significant hematite together with quartz, mica, montmorillonite, and amorphous components.

The mineralogical spectrum of the Upper Cretaceous (Campanian) sediments at Site 316, Cores 20 to 30 (630 to 837 m) seems to be most easily matched with the stratigraphic section in Hole 315A from 830 to 870 meters. The dominance of calcite (60% to 90%) is conspicuous in all greenish and brownish layers. Fine-grained lutite portions of graded layers contain the highest amounts of calcite, and the lowest is in a thick volcanogenic breccia bed (316-28-1, see Figure 3 and Plate 3) where it occurs as vug fillings, sparry cement, and rare fossils. Quartz content remains low, less than 3%, except in a brownish silt (705 m) which also showed a trace of dolomite. K-feldspars are an important constituent of coarse sandy layers and the breccia horizon, but are common in most samples. Plagioclase seems to be everywhere subordinate to K-feldspars. Analcite and traces of gibbsite were only detected in the volcanic breccia, which suggests that they are confined to the vesicle fillings and not formed in situ as at Site 317 (see Jenkyns, this volume). Montmorillonite is dominant over micas in the clay fractions.

CLAY MINERALOGY

Clay minerals in Cretaceous volcanic sediments (Cores 315A-22 to 30) occur as a replacement product of vesicular glass, as pseudomorphs after mafic minerals, and as intergranular matrix. The contact of clay minerals with altered glass is commonly fuzzy to embayed. Samples from cores just overlying the basement commonly have altered volcanic grains surrounded by a thin rim of highly birefringent, light greenish clay, possibly illite (celadonite). Commonly, this is accompanied by a rim of radial montmorillonite and an infilling of intergranular space with randomly oriented greenish montmorillonite (see Plate 1, Figure 7; Plate 4, Figures 3 and 7; and Plate 8, Figure 4). Based on EDAX and microprobe results, most of the clay minerals observed belong to the Fe-bearing montmorillonite family. Although many clay minerals have been redeposited to form the lutite fraction of turbidites, many appear to have formed from in situ alteration of volcanic grains, especially those from the coarser basal sections of the graded beds.

Several samples from K-feldspar-bearing sand layers were subjected to further X-ray analysis. Figure 4 compares two typical X-ray traces of bulk powder samples from near the bottom of Hole 315A and Site 316. A Phillips diffractometer with CuKα radiation and Ni filter run at 1° 2θ/min was used. Note that in the large *d*-spacing range the clay mineral spectrum is represented by broad asymmetric peaks of montmorillonite and mixed-layer minerals. Chlorite and illite peaks, when present, are suppressed by the abundance of smectites. Minor peaks rising from the shoulders of the 12.0 to 16.0Å spectrum suggest that the clay mineral populations are grossly inhomogeneous. Melson and Thompson (1973) emphasized that this was apparently characteristic of clays formed by the submarine weathering of basaltic sediment. Their study of the alteration of alkaline basalts from the Atlantic sea floor near St. Paul's Rock showed that the clay minerals were also a sink for potassium. The absence of a basal reflection around 10.0Å led them to conclude that the clay mineral phase best be termed K-smectite.

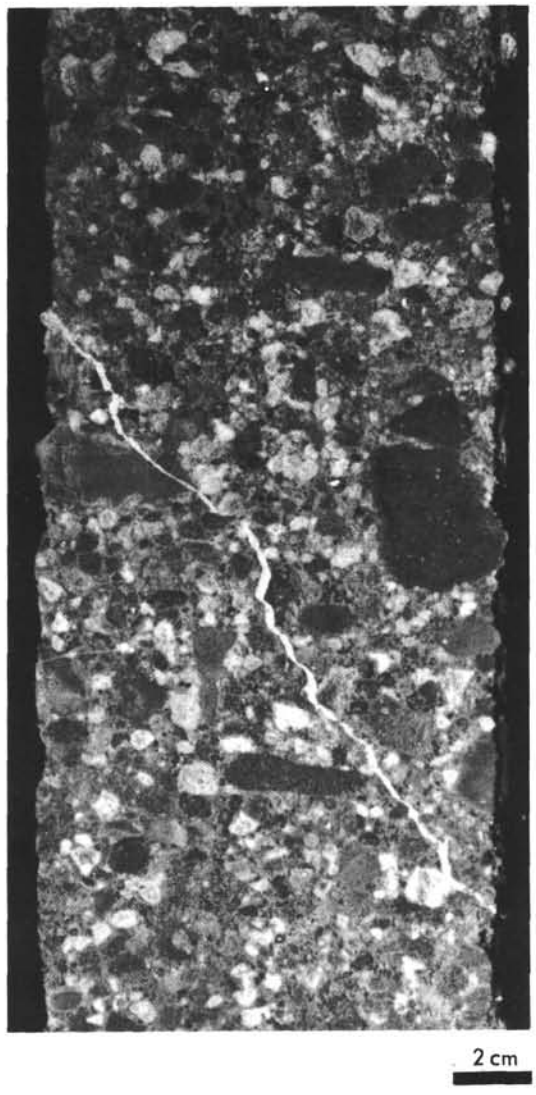

Figure 3. *Volcaniclastic breccia bed (2.5 m thick) 316-28-1. Subrounded to angular, light green clasts of altered vesicular glass with dark clasts of aphyric basalt and volcanogenic clay pebbles. Cut by a light yellowish-green, diagenetic montmorillonite vein.*

In order to better define the clay phases present in sand layers from Hole 315A and Site 316, three samples were size separated and the fractions were X-rayed. Samples were first disaggregated ultrasonically and sieved to 63μ. Sediment suspensions of the less than 63μ fraction were decanted after 10 min and 24 hr. Finally, aliquots were taken from the fine colloidal suspensions. Silt and sand fractions were crushed and decanted. A pure silicon standard was added and oriented mounts prepared for all splits. Samples were also glycol treated and heated to 550°C. Similar patterns were obtained from all three samples. A typical composite X-ray diagram is presented in Figure 5. The following conclusions can be drawn from these results: (1) The finest

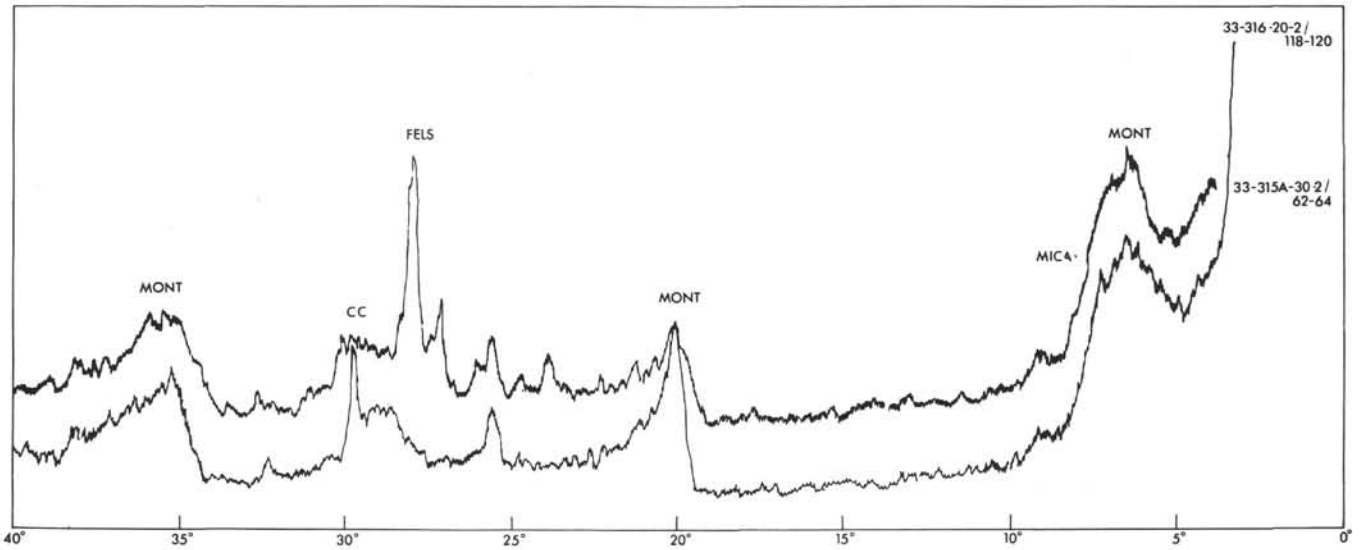

Figure 4. *Comparison of bulk X-ray diffraction results from typical volcanogenic sediments from Hole 315A and Site 316.*

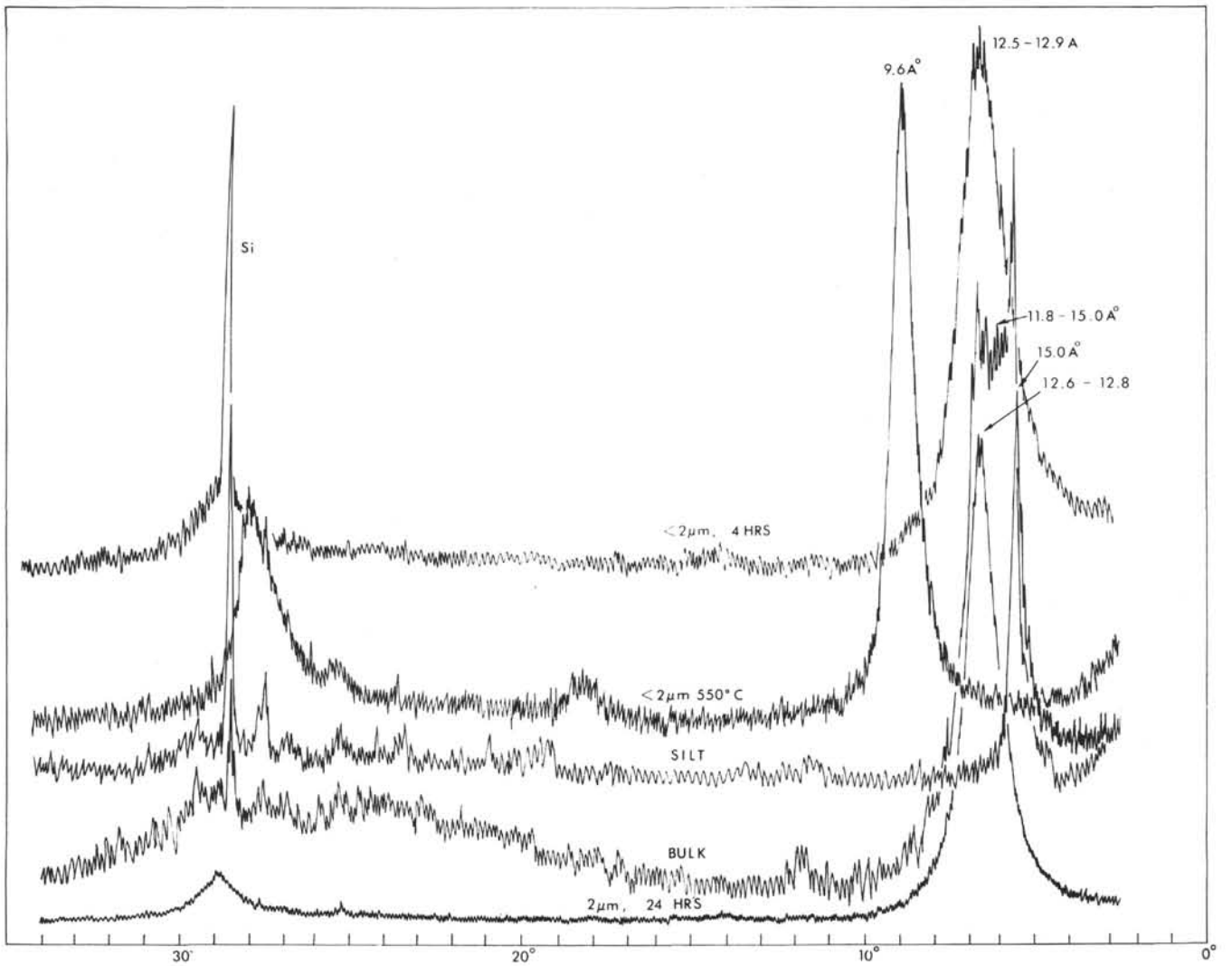

Figure 5. *Clay mineral X-ray diffraction results from separate size fractions from Sample 315A-29-2, 22-26 cm, a greenish-gray volcanic sand.*

grain size (<1μm) is dominated by a mixed layer phase with a well-defined peak.at 12.6Å. The peak collapses to around 9.6Å on heating and expands to 17Å with ethylene glycol suggesting an illite/montmorillonite mixed-layer clay. (2) The silt and sand grain-size fractions consist primarily of a well-defined 14.8 to 15.1Å peak indicative of montmorillonite plus a trace of chlorite. (3) Strong background and scatter indicate the presence of a considerable amount of iron with the clays. According to microprobe and energy-dispersive analysis, some iron and titanium is contained in the clay mineral phases either as nontronite or celadonite.

CHEMISTRY OF SEDIMENTS

Four samples representing varied lithologies were analyzed for trace elements and major oxides. The results are presented in Table 1. X-ray diffraction powder sample runs were made to correlate chemistry with mineralogy. Sample 19 was extracted from brownish claystones rich in fish debris from near the Cretaceous/Tertiary boundary. This was a control sample representing a deep-sea pelagic clay suite. The other samples are derived from the zone of unusual, colorful interlayers of sediments from 315A-28-3. Only Sample 22 (315A-29-2) is representative of typical graded volcanogenic sediments from basal parts of Hole 315A. The X-ray diffraction results are tabulated below:

315A-15-2, 110-115 cm Paleocene brownish-black claystone	Quartz + calcite dominant/ micas, montmorillonite, cristobalite, clinoptilolite, plus diverse traces (barite?)
315A-28-3, 82-85 cm Campanian greenish-black chert	Quartz dominant/mica abundant/trace feldspar and others
315A-28-3, 72-78 cm Campanian greenish volcanogenic claystone	Quartz + mica dominant/ montmorillonite and diverse traces
315A-29-2, 22-26 cm Campanian greenish volcaniclastic siltstone	Montmorillonite + feldspars (plagioclase + K-feldspar) abundant/chlorite and pyrox- ene (?), and traces of others

Chemical data were compared to results from metalliferous basal sediments on the East Pacific Rise (e.g., Cronan, 1972). Even cursory examination shows that the data have little similarity with ridge-crest basal sediments (see discussion by Jenkyns and Hardy, this volume).

Silica values are high in Samples 20 and 21 apparently as a result of silicification in claystones. Radiolarian molds of quartz were noted in these sediments. High potassium values correspond to the presence of mica minerals (iron-bearing illites ?). Volcanic sand results (Sample 22) are similar to other studies on weathering of basalts (Hart, 1970; Melson and Thompson, 1973; Stewart et al., 1973; and Bass et al., 1973). Iron, silica, potassium, and titanium are enriched. Calcium, sodium and aluminum appear depleted. This is reflected by the presence of replacement K-feldspars and by the composition of the clay phases.

DIAGENETIC K-FELDSPARS

Because the classification of alkaline volcanic rocks is partly dependent on the modal feldspar composition, a check of the exact composition and structural state is essential to the understanding of the alteration history of volcanics. Routine X-ray diffraction analysis of the volcanogenic sediments from Hole 315A and Site 316 revealed numerous occurrences of layers with up to 60% K-feldspar. Jackson et al. (this volume) failed to find any K-feldspars in the basalt flows cored in Hole 315A. Bass et al. (1973) noted, on the other hand, the presence of both diagenetically formed K-feldspars and primary K-feldspars in volcanic rocks and sediment from Hole 165A. Some thin sections of presumably diagenetic K-feldspar from Hole 315A are illustrated and described in Plates 5 and 7. We do not know, however, whether all the K-feldspars reported from basal sediments in Hole 315A and Site 316 are replacement products.

TABLE 1
Bulk XRF Chemistry of Some Hole 315A Cretaceous Sediments

	19	20	21	22
SiO_2	55.29	84.31	75.66	52.37
Al_2O_3	6.87	1.35	4.96	11.72
Fe_2O_3	7.90	5.40	9.65	9.82
MgO	2.49	1.13	1.99	6.35
CaO	9.39	2.98	1.03	2.84
Na_2O	1.55	0.55	0.84	1.45
K_2O	1.45	1.23	2.16	1.90
TiO_2	0.57	0.18	0.62	2.15
S	0.20	0.34	0.00	0.52
P_2O_5	1.24	0.88	0.11	0.27
Subtotal (%)	86.94	98.35	97.02	89.39
MnO (%)	0.91	0.29	0.39	0.72
Pb (ppm)	120	0	7	8
Cu (ppm)	727	12	51	119
Ni (ppm)	196	20	15	81
Cr (ppm)	51	24	34	77
Co (ppm)	62	40	50	32
Ba (ppm)	5483	0	61	66
Nb	21	10	15	35
Zr	186	28	116	264
Y	274	112	22	54
Sr	708	83	104	339
Rb	66	59	90	45
Zn	420	45	396	902

Note: 19 = 315A-15-2, 110-115 cm; upper Paleocene brownish-black claystone; 20 = 315A-28-3, 82-85 cm; lower Campanian (Santonian?) greenish-black chert nodule in a volcanogenic sediment; 21 = 315A-28-3, 71-78 cm; lower Campanian (Santonian) greenish claystone volcaniclastic; 22=315A-29-2, 22-26 cm; lower Campanian (Santonian) greenish-gray volcanoclastic sandstone with K-feldspar.

STRUCTURAL STATE

Wright (1968) discovered an empirical linear relationship between the a, b, c crystallographic axis and certain X-ray diffraction peaks from K-feldspars. By measuring the distance between these peaks, the structural state can be clearly determined. Three samples from sandy layers containing replacement K-feldspars were selected from the lowest two cores, 29 and 30. Samples were disaggregated and sieved to 63μ. The sand-sized fraction was crushed and nonoriented powder samples with a silicon standard were run at 1/4°

2θ/min on a Phillips CuKα diffractometer. The results for these samples were the same as given below:

Diffraction Peak Indexes	2θ value ±0.3
201	21.06
060	44.71
204	50.75
002	27.63
113	38.85

Using the figures in Wright (1968) this indicates a slightly anomalous orthoclase or intermediate microcline with a structural state near the standards: Benson orthoclase and SH1070 or Spencer adularia. It was apparent from the diagrams that this was the only K-feldspar phase present in the sand fraction of these samples.

Another method to determine the character of K-feldspars is given in Goldsmith and Laves (1954). These authors introduced the term triclinicity to express the gradation between monoclinic feldspar and maximum microcline. It is based on the amount of splitting visible in the 130 and 131 reflections. Applying this method to the diffractograms for Samples 315A-29-2, 22-25 cm, 315A-30-2, 92-96 cm, and 315A-29-1, 44-46 cm resulted in a triclinicity value of 0.2. Both 130 and 131 showed clear evidence of splitting. This would thus imply that the K-feldspar in these samples is an intermediate microcline of moderate Al-Si ordering, in fact almost a monoclinic K-feldspar. Both methods are in agreement that these K-feldspars are nearly monoclinic. However, Smith (1974) has pleaded that microcline be the name given to any K-feldspar with measurable triclinicity and this practice is followed here.

MICROPROBE ANALYSIS

The samples discussed above were also examined with an ARL model SEMQ microprobe. Beam width was approximately 2μ and beam strength about 15 Kev. Eight elements (K, Si, Ti, Na, Ca, Fe, Mg, and Al) were analyzed using the standards orthoclase (K, Si, Al), olivine (Fe, Mg, Ti), bytownite (Ca), and albite. Standards were chosen to correspond with the sediment and provide good first-order data. Corrections were made automatically for deadtime, drift, and background. Analysis was terminated by an electrical contact rupturing in the Al and Si spectrometer. The samples, all from greenish-black graded sands, were prepared by first ultrasonically cleaning the sand-size fraction and hand-picking clear and cloudy white grains presumed to be K-feldspars. Some of the grains were reserved for scanning electron microscopy, and others were prepared as transparent, polished grain mounts for the microprobe (see Figure 6). Results are tabulated in Table 2.

All the feldspar grains analyzed are purest end-member compositions with negligible substitution of Na or Ca. There were no exceptions although we recognize that the optical selection may have prejudiced the results. Future work on polished thin sections will reduce this possibility. It is premature to conclude that all the K-feldspars in all the samples are pure-potassium, intermediate microclines.

Cathode Luminescence

Based on Kastner's (1971) criteria for recognizing authigenic feldspars, we checked for cathode luminescence on all the microprobe grain mounts. The orthoclase standard exhibited a circle of bright blue fluorescence more than 10 times the beam width. In contrast, all of the feldspar grains showed little or no fluorescence at the same energy levels. At maximum, a dull, faint creamy white pinpoint fluorescence was observed in some grains with a diameter roughly equivalent to the beam width. Kastner (1971) considered this to be a good indication of low-temperature formation.

SURFACE MORPHOLOGY OF VOLCANOGENIC GRAINS

Using a Cambridge scanning electron microscope with energy-dispersive X-ray analyzer (EDAX), we examined the surface morphology of some sand-sized volcanic grains taken from layers rich in diagenetic feldspars. Most clay minerals exhibited a fabric of wavy and irregularly crumpled sheets characteristic of the smectite group (Borst and Keller, 1969). Some devitrified volcanic glass grains (see Plate 9 and Plate 10, Figure 5) show surface coatings of montmorillonite or mixed-layer minerals and internal alteration products in the form of clean sheaves. These contain Si, Fe, Mg, Al, and some K, possibly as a chlorite mineral. EDAX measurements on the surfaces of some irregular clay minerals indicate that K and Fe plus some traces of titanium appear to be a part of the clay structure. Some vesicle linings show a coating of new montmorillonite growth. Other fragments exhibit a spalling texture in the interior altered to twisted sheaves of clay minerals. Solutions apparently alter the fragments rapidly along microfractures. The scanning micrographs underline the importance of microporosity as a control on the extent of diagenesis. Mafic minerals and volcanic glass spherulites (Plate 14) appear to alter in situ to clay minerals which clog the pore space. These clays have a more irregular structure than those encountered on K-feldspars and suggest that clay mineral compositions may be tied to the composition of the host grain.

Results of surface textural studies on K-feldspars are extensively discussed below and in Plates 6, 10, 11, 12, and 13.

DISCUSSION

Diagenetic K-Feldspars

The existence of chemically pure K-feldspar crystals (intermediate microcline) in the Cretaceous volcanogenic sands from Hole 315A and Site 316 along the Line Islands poses problems as to their origin. Physically these subidiomorphic crystals appear to have undergone various stages of destruction. Some crystals are euhedral, while others are anhedral. Some grains show signs of broken edges and others have well-rounded edges. All can be found together in the same sediment sample and include in their numbers hollow-centered intermediate microcline crystals with irregular, step-like surfaces in the cavity interiors. Many grains contain in-

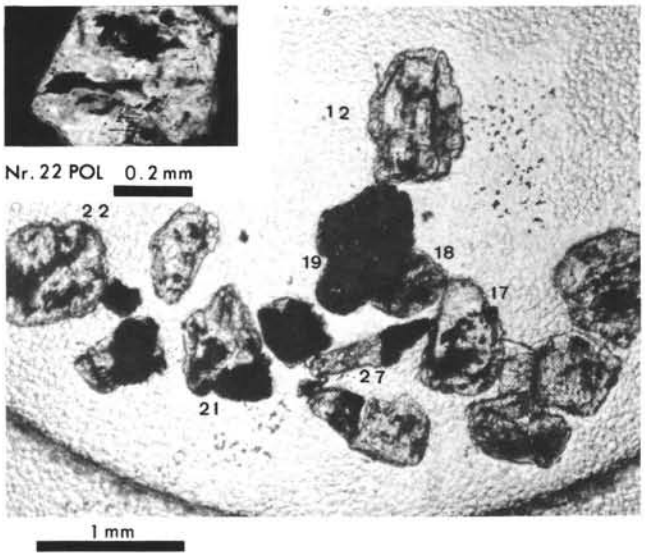

Figure 6. *An example of a carbon-coated polished grain mount of K-feldspars (Sample 315A-29-2, 22-26 cm) selected for microprobe analysis. Viewed in transmitted plane-polarized light. Numbers correspond to the analysis points listed in Table 2. Number 19 is a clouded white grain while the others are mostly clear. Black patches are mostly clay aggregates. Some grains contain cavities with idiomorphic outlines. Note the micrograph inset of grain 22 showing a homogeneous extinction.*

clusions of altered basaltic glass, high birefringent heavy minerals, or zeolites. (See Plates 5 and 6.)

Microscopically, in plane polarized light the crystals appear in general to be homogeneous. Many exhibit simultaneous extinction, at least around the rims. Some have patchy and irregular extinction, possibly due to the inheritance of a former crystal twinning or as a result of replacement in stages. A few rare crystals in the lowermost sediments (Core 30) show an irregular gridiron extinction pattern, a possible relic of anorthoclase. Twinning rarely occurs.

The compositionally pure K-feldspar grains do not show significant cathode luminescence. This observation complies with Kastner's (1971) criteria for low-temperature formation. However, a combination of chemical purity, little twinning, and lack of cathode luminescence is enough to suggest an authigenic or secondary metasomatic replacement mechanism as a mode of origin. Therefore, a high-temperature, volcanic origin for the K-feldspar can almost certainly be excluded.

What then is the mode of origin for the K-feldspar in the volcanogenic sands? Textural patterns observed in thin sections definitely imply a pseudomorphic replacement rather than authigenic growth from the matrix. We propose that there are three possibilities for this replacement mechanism. Although K-feldspar is present throughout the volcanogenic section, the conclusions here apply only to Cores 28, 29, and 30. Skeletal or clearly replacement K-feldspars were not observed in thin sections above these cores. No microprobe data are yet available.

Case 1: The K-feldspar was an early in situ replacement of plagioclase in the basalts before transport. This origin could explain the worn appearance of some of the K-feldspar grains. On the other hand, it does not explain the stratigraphic anomalies. In a vertical profile there is a nonhomogeneous distribution of K-feldspars, especially those with replacement textures.

Although the basalts cored in Hole 315A appear to have alkaline affinities (Jackson et al., this volume), they do not contain modal K-feldspars. There is also a qualitative observation from X-ray data that plagioclase abundance correlates negatively with K-feldspar. Detrital, single plagioclase laths were not observed in thin sections of volcanogenic sand containing pure K-feldspars. We have noted that the pure microcline feldspar concentrations seem to be closely associated with zones of colorful interlayers (e.g., Core 28, Section 3 and Core 29, Section 1), which themselves appear to be a solution-alteration feature.

Because the volcanogenic sediments are redeposited, the presence of replacement K-feldspars in the original basaltic rocks cannot be ruled out. This, however, would imply a significant time lapse between eruption, alteration, and transport of the sediment. The hyaloclastic texture of the sediment suggests that the volcanogenic material was neither highly altered before redeposition nor was the distance of transport very great. We tend, therefore, to believe that pure K-feldspar was not directly derived from the volcanic source area. Other K-feldspars, including some anorthoclase, may have been derived from nearby alkalic cones.

Case 2: K-feldspar crystals are pseudomorphic replacements of plagioclase or other felsdpars after deposition. This mechanism would explain the frequent occurrence of K-feldspar grains with a plagioclase morphology (see Plate 10, Figure 1) and the existence of a few rare composite feldspar crystals (see Plate 7, Figure 5). The mutual exclusivity of the feldspar phases could be a result of a nonhomogeneous, horizontally stratified distribution of the potassium-rich solutions necessary for a chemical replacement. At DSDP Hole 165A and Site 192 a K-feldspar mineral assemblage similar to that described in this paper was observed. This implies further that this replacement mechanism is not a localized but a regional phenomenon.

Case 3: A third possible mode of formation is that some K-feldspar may have precipitated directly from a hydrothermal solution filling the voids and replacing the matrix. The hollow crystals could form as the microcline crystallized on the surface of the voids and grew progressively inward. However, if this third mechanism were the predominant one, a greater abundance of euhedral crystals should be found. A few rare hollow K-feldspar grains were found encompassing vesicles in breccia clasts from Site 316 (see Plate 3, Figure 5) and Bass et al. (1973) illustrate examples of euhedral K-feldspar rims around void space in basalt samples. An alternate explanation may involve the complete or partial resorption of the original feldspar phenocryst parallel with its replacement. Evidence of extreme alteration phases within the cavities is illustrated in Plate 6 where low silica (gibbsite?) products are present.

Synthesis of the data presented in this paper leads us to believe that the formation of the compositionally pure K-feldspar is probably a result of a combination of Cases 2 and 3. Together, these two mechanisms best ex-

TABLE 2
Microprobe Analysis of K-Feldspar Grains

	K	Si	Al	Na	Ca	Fe	Mg	Ti	Cation Total (%)
Feldspar									
Orthoclase standard	16.58	64.55	18.36	0.06	0.0	0.0	0.0	0.0	100.
12.1 Fresh surface, clear grain	15.75	60.76	17.96	0.09	0.0	0.02	0.0	0.0	94.5
12.1 Inner edge	15.85	64.12	18.45	0.05	0.0	0.0	0.0	0.03	98.49
12.3 Inclusion	13.07	65.34	19.87	0.02	0.0	0.04	0.0	0.0	98.35
12.4 Free-floating crystal inclusion	16.52	63.98	18.91	0.04	0.0	0.01	0.0	0.02	99.5
19.1 Milky subhedral grain	16.17	62.25	18.36	0.07	0.02	0.06	0.0	0.13	97.07
12-1 Stand reset	13.8	63.3	18.62	0.08	0.02	0.0	0.02	0.01	95.85
17.1 Clean surface	15.07	63.9	18.81	0.06	0.01	0.02	0.0	0.0	97.0
22.2 Clean surface	11.57	62.83	18.78	0.13	0.0	0.04	0.01	0.0	96.0
22.3 Crossed prisms	14.31	57.61	16.76	0.08	0.03	0.24	0.21	0.02	89.2
25.1 Clean outer edge	14.83	64.73	19.40	0.01	0.03	0.2	0.0	0.0	99.0
9.2.1 Cloudy along cleavage	13.33	–	–	0.04	0.0	0.02	0.0	0.0	–[a]
9.2.2 Fresher area than above	14.41	–	–	0.03	0.0	0.03	0.0	0.0	–[a]
9.6.1 Clear	13.07	–	–	0.04	0.0	0.01	0.0	0.0	–[a]
3.1 Clear without cleavage	13.68	–	–	0.07	0.01	0.0	0.0	0.0	–[a]
12.1 Repeated/control	14.58	–	–	0.07	0.0	0.02	0.0	0.0	–[a]
Accessory Inclusions and Alteration Products Associated with Feldspars									
19.2 Extreme grain edge alteration	5.89	33.78	11.74	0.16	0.49	2.32	2.39	21.83	78.0
27.1 Clear prismatic inclusion	7.23	65.79	19.34	0.03	0.0	0.0	0.0	0.0	92.3
27.2 Greenish clay clump in cavity	13.88	51.08	15.31	0.08	0.21	1.24	1.34	0.06	83
18.1 Outer edge of altered grain	11.07	49.29	14.27	0.32	3.05	1.16	1.49	1.53	82
17.2 Cavity lining	14.38	62.6	14.73	0.05	0.44	4.5	4.65	0.1	101
17.3 Outer surface alteration (chlorite)	0.31	34.32	6.8	0.17	1.63	13.09	14.88	0.0	71.
22.1 Clay clump in cavity	0.16	34:2	0.31	2.73	2.86	0.05	1.54	0.0	41 (?)[b]
25.3 Authigenic clusters	0.21	30.37	6.35	0.15	1.07	14.06	11.46	0.02	63[a]
11.1 Authigenic mineral	3.8	16.65	4.75	0	0	0	0	0	25[a]

[a]Measurements made with a defective Al/Si spectrometer and therefore are left blank.

[b]Measurements which do not sum to nearly 100% may be due to (1) high water content in the mineral phase, (2) low beam current due to poor polish, (3) additional significant elements, (4) poor conduction through the carbon coating due to isolation of the grains by pits, (5) combination. Grains were numbered consecutively in a single sample and the decimal refers to a second or third measurement on the same grain.

plain all the observed physical and chemical properties of the K-feldspar. The chemically pure microcline is most probably the product of the interaction of potassium-enriched solutions with the volcanogenic sands. The volcanic sands are found adjacent to an alkalic province and late-stage alkalic volcanic emanations may have been active shortly after deposition. It becomes difficult to determine the exact origin of these solutions as there is no direct evidence available. Potassium enrichment in altered basalts is now well documented in the deep-sea environment (Moore, 1966; Hart, 1970; Melson and Thompson, 1973). However, this enrichment is not commonly encountered as K-feldspars. This leads us to conclude that the potassium in the altering solutions may have a more complex origin than simply trapped sea water.

K-Feldspar Surface Morphology and Subsequent Alteration

Compositionally pure K-feldspar crystals formed at low temperatures represent a very stable phase. It follows that alteration of these crystals in a submarine-weathering environment would be an extremely slow process. As a result, the microcline grains found in the volcanic sands in Hole 315A present a window in which to view some aspects of the changes that occur during the initial stages of low-temperature diagenesis of feldspars. Even after 60 m.y. some K-feldspar grains show only moderate surficial alteration. From our scanning electron microscope study of the crystal surfaces we have been able to distinguish three early stages in the breakdown of the feldspar framework to form phyllosilicates.

The three stages of early alteration that we postulate may be progressive or may be simultaneous. Commonly, the first two stages occur on the same crystal. All three stages are part of the initial breakdown of the feldspar surface.

Stage 1 consists of an elongate etching most pronounced on the (100) and (010) surfaces (see Plate 11, Figures 1 and 4) and a leaching out of the silicate framework structure (see Plate 12, Figures 1, 2, and 3; Plate 13, Figure 2). The leaching appears to leave gaps in the surfaces which are criss-crossed and spanned by bridge-like supports. These gaps may be associated with the crystal lattice directions having the lowest free energy. There is also a possible allophane coating growing on the surface of the crystals (Plate 13, Figure 6 or Plate 11, Figure 4), but it is impossible to distinguish poorly crystallized allophane from an amorphous iron-oxide coating.

Stage 2 alteration consists of the initial formation of phyllosilicates with moderate to well-defined crystal structures. The newly formed clays appear to lift or peel

up from the crystal surfaces as the three-dimensional framework of the microcline is destroyed (Plate 11, Figure 3; Plate 14, Figures 5 and 6; Plate 12, Figure 2).

In Stage 3 the phyllosilicate development occurs as a dense continuous surface coating on the K-feldspar. This dense, mat-like reaction product appears to be a monomineralic layer that can be removed from the original crystal in sheets (Plate 12, Figures 4, 5, and 6). The surface coating of clays on this grain was undoubtedly cracked and broken loose during the ultrasonic separation of the grains. The crystal surface underneath the phyllosilicate sheet shows evidence of stepwise Stage 1 etching and leaching (Plate 12, Figures 5 and 6). This may indicate that the three early stages of alteration are progressive.

With the first stage of alteration the surfaces are structurally weakened by the processes of solution and hydration. During the second stage discrete phyllosilicate crystals begin to grow on the disrupted surfaces utilizing the lattice structure of the K-feldspar as a preferred site of growth. With continued phyllosilicate growth, dense layers form over the surface of the crystals in Stage 3. Further alteration proceeds inward toward the center of the crystal with each subsequent fresh surface of the feldspar grain being transformed in a series of three stages.

Alteration features similar to our proposed Stages 1 and 2 have been reported by Divis and McKenzie (in press). They conducted hydrothermal experiments to study the alteration of feldspathic sands in contact with saline solutions under conditions approximating burial depths of 3 to 10 km and temperature ranges of 200° to 300°C. Scanning electron micrographs of the orthoclase crystals reacted for periods of approximately one month showed: (1) elongated solution features, (2) well-formed discrete phyllosilicate crystals lifting up from the crystal surface, and (3) initiation of a random intergrowth of the phyllosilicate cover on the orthoclase surface. It appears that phyllosilicate crystals formed under both experimental and natural conditions utilize the surface of the K-feldspar as a preferred site for nucleation and growth.

The development of phyllosilicate minerals from feldspars has been extensively studied, particularly from a theoretical viewpoint. DeVore (1957) theorized that the feldspar structure was a dominant control on phyllosilicate nucleation and growth. He proposed that phyllosilicates grow utilizing surficial tetrahedral groups produced during the destructive hydration of the feldspar crystals. Helgeson (1974) further visualizes that this incongruent hydrolysis proceeds stepwise with an inward development of a series of monomineralic zones. These zones would appear as surface coatings or layers on the feldspar grains. Alteration proceeds with continued outward diffusion of material through the surface layer until the feldspar is totally destroyed.

The relationship between probable and natural mechanisms of phyllosilicate formation is not clearly developed. It is difficult to extrapolate from theoretical models dealing with chemical reactions on a molecular level to macroscopic observations. Nevertheless, our description of the three early stages of K-feldspar alteration is quite possibly related to the theoretical picture of phyllosilicate development.

Possible Regional Significance of Pure-phase, Diagenetic K-feldspar

In an earlier study of regional feldspar occurrences, Peterson and Goldberg (1962) used X-ray methods to determine the distribution of feldspars in cores from pelagic sediments in the South Pacific. They found that plagioclases of intermediate composition were the dominant phase. K-feldspars were rare and were represented by minor amounts of sanidine and anorthoclase. Microcline was reported to be absent from all their samples. Thus, could the presence of intermediate microcline in the Line Islands volcanogenic sediments be considered an anomaly?

In order to form a perspective, we will review some previous studies on presumably diagenetic K-feldspars associated with oceanic volcanic sediments. Matthews (1971) reported the replacement of calcic cores of plagioclase by orthoclase in his discussion of submarine weathering of slightly alkaline tholeiites. In contrast, the sodic rims of plagioclase were altered to montmorillonite. Other Atlantic sediments from DSDP Leg 11 described by Lancelot et al. (1972) contained authigenic sanidine replacing volcanic glass shards. These were associated with brightly colored red and green interbeds just above the basalt at Site 105. However, their prismatic habit contrasts with pseudomorphic K-feldspar crystals from Hole 315A.

Secondary pseudomorphic replacements of plagioclases by pure K-feldspar phases have recently been described from a number of Pacific DSDP localities. Commonly, these have been in Upper Cretaceous volcanogenic sediments or rocks associated with seamounts having slight to moderately alkaline compositions. For instance, Bass et al. (1973) described the replacement of calcic plagioclase cores by pure K-feldspar in Leg 17 Cretaceous basalts. These authors envision a zeolite metamorphism at Site 165 but with a later diagenetic replacement of Ca-plagioclase by K-feldspar after cooling. Evidence for an early conversion to pure monoclinic (?) K-feldspar is given by the K/Ar age of 58 m.y. obtained on a split of pure K-feldspar from Site 169. DSDP Leg 32, Site 313, recovered Campanian sediments which contained K-feldspars in foram chambers. Stratigraphic similarity to 315A would lead us to predict that the basaltic rocks and sediments contain pseudomorphic K-feldspars (Larson, Moberly, et al., 1974).

Stewart et al. (1973) were surprised to find plagioclase crystals with K-feldspar cores in Upper Cretaceous (Maestrichtian-Campanian) alkaline basalts from the Meiji Guyot, DSDP Site 192. They concluded that the K-feldspar was secondary since it could not have crystallized in equilibrium with the associated labradorite. A late-stage differentiate was excluded by the lack of phenocrysts in the glassy rinds. Therefore, they attributed the origin to solutions produced during the alteration of the basalts. The limitation of the occurrences of K-feldspars to the coarse-grained sections implies that porosity is an important controlling factor. The compositionally pure K-feldspars they tentatively

identified as sanidine, having a morphology slightly different from many Site 315A intermediate microclines but may actually be equivalent. The crystal habit is commonly an exact replica of an elongate plagioclase lath.

Skeletal laths of labradorite which could also have been the precursors of K-feldspar pseudomorphs were described by Yeats et al., 1974. These feldspars were found in a Cretaceous (Campanian) basalt core from DSDP Leg 16 in the Central Pacific The laths were filled with glass, pyroxenes, and opaque minerals. Anomalously low K/Ar dates suggested that potassium replacement had been active.

It has been postulated (e.g., Winterer, this volume) by a reconstruction of Campanian ocean crust that the Line Islands sediments may have an equivalent facies in the Caribbean area. Campanian volcanic sequences with some similarities to Hole 315A and Site 316 have been described by Donnelly and Nalli (1973). They also noted the presence of authigenic, pure K-feldspars associated with the Santonian-Campanian volcanic sediments at several DSDP Leg 15 sites. Again, there are discrepancies with the morphology of these K-feldspars and those of Hole 315A. The Caribbean K-feldspars have euhedral shapes, are flattened on (010), and contain abundant inclusions. By a process of elimination Donnelly concludes that these crystals have an authigenic origin.

It is too early to generalize on the regional ramifications of pure K-feldspar occurrences in Upper Cretaceous volcanogenic rocks in the deep sea. The physical-chemical conditions prevailing during the formation of pure K-feldspars in volcanogenic sediments are still poorly understood. A confusion of terminologies and lack of exact phase identification has perhaps hampered the recognition of a widespread presence of pure intermediate microcline pseudomorphs. We note from a comparison with previous works that a variety of modes of occurrence are postulated for the K-feldspars.

Still, some parallels are seen which indicate that the K-feldspar occurrences noted to date are: (1) in association with alkaline provinces around seamount groups, (2) common in Pacific volcanics of Upper Cretaceous age, (3) commonly in association with potassium-rich clays, and (4) commonly in association with coarser grain sizes and porous zones. The burial depths vary widely, suggesting the overburden is not a controlling factor in the formation of K-feldspars. Temperature estimates for the formation, also, vary widely ranging from normal seabottom conditions (Matthews, 1971) to hydrothermal solutions (Stewart et al., 1973). The influence of temperature remains an unanswered question.

We consider the mechanics of K-feldspar replacement to be a possible potassium equivalent of spilitization. DeRoever (1942) introduced the term *poeneites* named after the river Noil Poene on the Island of Timor in the Indonesian Archipelago. There, he recognized extensive metasomatic K-feldspar replacement of calcic plagioclases in olivine basalts of Permian age. In his petrographic study he also described anorthoclase crystals which showed considerable resorption and corrosion effects. He was convinced that the process must be widespread and named the process "adularization," which was at that time referring to orthoclase. We suggest that this K-enrichment mechanism, not yet well known from basaltic deposits on land, be termed *poeneitization* after DeRoever's (1942) classic study to denote the differences between this process and more common spilitization.

Diagenesis

Strong textural and mineralogical evidence exists that the Cretaceous volcanogenic sediments cored on Leg 33 were derived by processes of alteration and weathering (halmyrolysis) of redeposited volcanic material. Much of the matrix in coarse-grained layers is considered to be of post-depositional origin. However, it is difficult to differentiate the roles played by temperature, burial, age, composition, and porosity in this alteration.

No heat-flow determinations were made on Leg 33, but using the usual heat-flow values an approximate temperature of 50° to 60°C might be expected at the base of Hole 315A. In Campanian-Santonian times local heat flow may have been high, but overburden was a maximum of 150 meters. The possibility of some local hydrothermal activity is hard to exclude. The occurrence of an aragonite-cement-bearing layer containing quartz, feldspar, and mica, in an otherwise calcium-poor environment, is a particular problem. Natland (1973) concluded that a similar layer from Site 183 may have been due to its fortuitous location in the vicinity of a local fumarole vent.

The progressive diagenetic alteration in argillaceous sediments of montmorillonites to mixed-layer assemblages and illite with depth has been noted by many authors (e.g., Weaver and Beck, 1971; Matter, 1974; Heling, 1974). The clay mineral assemblage we observed at the base of Hole 315A and Site 316 contained a mixture of discrete montmorillonite, potassium mixed-layer clays (illite/montmorillonite), traces of illite (celadonite), and chlorite. This is not inconsistent with a diagenetic assemblage expected for a depth of 800-1000 meters and temperatures of 50° to 70°C (Heling, 1974). However, we believe that there may have been several generations of clay mineral formation. Recent studies indicate that the same mineral assemblage may be formed early in the depositional history. For instance, many parallels were found between our study and the results of Melson and Thompson (1973). Their study of the halmyrolysis of dredged basalts reported the presence of clay minerals enriched in potassium and somewhat in titanium. Their K-smectites could be the same type of mixed-layer clay formation.

Hay and Iijima (1968) studied the conversion of volcanic glass to palagonite. They concluded that at normal sea-water temperatures submarine devitrification took place rapidly but is closely related to compositional variations and the presence of microfractures as solution conduits. They also recorded the presence of mixed-layer clays. Similar results were reported by Moore (1966) who also noted enrichment of Ti, Fe, and K in recent submarine basalts. The application of these results to the volcanogenic sediments from Hole 315A and Site 316 suggest that they may have been largely converted to palagonite and diverse smectite minerals within a few million years. We found that parts of some volcanic

glass grains, isolated from circulating solutions, had escaped destruction. Porosity of the initial sediments is apparently a controlling factor. The clays have a tendency to fill in available pore space, which may have resulted in a decreased transportability of solutions through the sands.

K-feldspar diagenesis has been discussed above. Calcite was not an important diagenetic mineral in the basal part of 315A nor were zeolites. They may be the result of leaching or original compositional variations leading to low CO_2 activities. In either case compared to Hole 165A with a zeolite metamorphic assemblage (Bass et al., 1973), the diagenetic assemblage in Hole 315A is impoverished. The fact that Hole 165A has 600 meters less overburden than 315A suggests that burial depth was not a critical factor.

CONCLUSIONS

Our study of Upper Cretaceous volcanogenic sediments from DSDP Leg 33 taken at Hole 315A and Site 316 along the Line Islands chain has revealed a complex alteration history. Diagenesis of these sediments does not necessarily show a linear progression with depth. Montmorillonite and mixed-layer clay assemblages may have formed during early halmyrolysis before significant burial as well as during progressive diagenesis throughout the sedimentary column. Temperature and burial may be important but age, porosity, seawater leaching, and even possible local hydrothermal activity must also be considered as controlling factors. The sediments have undergone an enrichment in K, Fe, Ti, and Si while being depleted in Na, Ca, and Al. This is reflected in both the clay mineral phases and the compositionally pure K-feldspar pseudomorphs recognized in the sediments.

The K-feldspar grains found in the basal volcanic sands were identified as chemically pure, intermediate microcline. Their physcial and chemical properties indicate that their mode of origin was most likely the result of early post-depositional, low-temperature metasomatic replacement of plagioclase or other feldspars and possibly void filling due to potassium-rich solutions from late-stage volcanic emanations, in situ devitrification of alkali glass, or from interstitially altered sea water. The slow, low-temperature alteration of the compositionally pure feldspar grains was described, and three stages in the early development of phyllosilicate minerals were discussed.

The apparent K-metasomatism is essentially the potassium equivalent of spilitization. Regional implications were drawn from the widespread occurrence of similar potassium-rich, diagenetic assemblages found in Upper Cretaceous volcanogenic sediments from other alkaline seamount sites in the Central and North Pacific realm.

ACKNOWLEDGMENTS

We are grateful to all our colleagues on DSDP Leg 33 for valuable discussions. Hugh Jenkyns and Dale Jackson were especially helpful with information and comments. Ron Hardy from Durham University kindly provided complete XRF analyses on four samples. We thank Helmut Frantz and Jack Rice for introducing us to the SEM and microprobe operations. Discussions about mineral alterations and feldspars with H.U. Nissen, Ken Hsü, and Dave Kersey were appreciated. Urs Gerber improved most of the photographs.

A potassium/argon date was kindly run by M. Lanphere and colleagues of the U.S. Geological Survey, Menlo Park on a pure K-feldspar split from Sample 315A-29-2, 22-26 cm. As further evidence confirming an early replacement mechanism, they report an age of 85 ±3 m.y. with excellent argon retention.

REFERENCES

Bass, M.N., Moberly, R., Rhodes, J.M., Shih, C., and Church, S.E., 1973. Volcanic rocks cored in the Central Pacific, Leg 17, Deep Sea Drilling Project. *In* Winterer, E.L., Ewing, J.I., et al., Initial Reports of the Deep Sea Drilling Project, Volume 17: Washington (U.S. Government Printing Office), p. 429-503.

Borst, R.L. and Keller, W.D., 1969. Scanning electron micrographs of API reference clay minerals and other selected samples: Int. Clay Conf. Proc., Tokyo, 1969, v. 7, p. 871-901.

Cronan, D.S., 1973. Basal ferruginous sediments cored during Leg 16, Deep Sea Drilling Project. *In* van Andel, T.H., Heath, G.R., et al., Initial Reports of the Deep Sea Drilling Project, Volume 16: Washington (U.S. Government Printing Office), p. 601-613.

DeVore, G.W., 1957. The surface chemistry of feldspars as an influence on their decomposition products: Clays Clay Minerals, v. 6, p. 26-41.

DeRoever, W.P., 1942. Olivine basalts and their alkaline differentiates in the Permian of Timor. *In* Brouwer, H.A. (Ed.), Geological expedition to the Lesser Sunda Islands, v. 4, p. 209-289.

Divis, A.F. and McKenzie, J.A., in press. Experimental authigenesis of phyllosilicates from feldspathic sands: Sedimentology, v. 22.

Donnelly, T. and Nalli, G., 1973. Mineralogy and chemistry of Caribbean sediments. *In* Edgar, N.T., Saunders, J.B., et al., Initial Reports of the Deep Sea Drilling Project, Volume 15: Washington (U.S. Government Printing Office), p. 929-961.

Goldsmith, J.R. and Laves, F., 1954. Potassium feldspars structurally intermediate between microcline and sanidine: Geochim. Cosmochim. Acta, v. 6, p. 100-118.

Hart, R., 1970. Chemical exchange between sea water and deep ocean basalts: Earth Planet. Sci. Lett., v. 9, p. 269-279.

Hay, R.L., and Iijima, A., 1968. Petrology of palagonite tuffs of Koko Craters, Oahu, Hawaii: Contrib. Mineral. Petrol., v. 17, p. 141-154.

Helgeson, H., 1974. Chemical interaction of feldspars and aqueous solutions. *In* McKenzie, W.S. (Ed.), Feldspars: Nato Advanced Study Institute, July, 1972 (Manchester), p. 184-217.

Heling, D., 1974. Diagenetic alteration of smectite in argillaceous sediments of the Rhinegraben (SW Germany): Sedimentology, v. 21, p. 463-472.

Kastner, M., 1971. Authigenic feldspars in carbonate rocks: Am. Mineral., v. 56, p. 1403-1442.

Lancelot, Y., Hathaway, J.C., and Hollister, C.D., 1972. Lithology of Sediments from the Western North Atlantic, Leg 11, Deep Sea Drilling Project. *In* Hollister, C.D., Ewing, J.I., et al., Initial Reports of the Deep Sea Drilling Project, Volume 11: Washington (U.S. Government Printing Office), p. 901-973.

Larson, R., Moberly, R., Bukry, D., Foreman, H.P., Garner, J.V., Keene, J., Lancelot, Y., Luterbacher, H., Marshall, M. and Matter, A., 1974. Leg 32, Deep Sea Drilling Project: Geotimes, v. 18, p. 14-18.

Matter, A., 1974. Burial diagenesis of pelitic and carbonate deep-sea sediments from the Arabian Sea. *In* Whitmarsh, R.B., Weser, O.E., et al., Initial Reports of the Deep Sea Drilling Project, Volume 23: Washington (U.S. Government Printing Office), p. 421-469.

Matthews, D.H., 1971. Altered basalts from Swallow Bank, an abyssal hill in the Northeastern Atlantic and from a nearby seamount: Phil. Trans. Roy. Soc. London Acad., v. 268, p. 551-571.

Melson, W.G. and Thompson, G., 1973. Glassy abyssal basalts, Atlantic sea floor near St. Paul's Rock: Petrography and composition of secondary clay minerals: Geol. Soc. Am. Bull., v. 84, p. 703-716.

Moore, J.G., 1966. Rate of palagonitization of submarine basalt adjacent to Hawaii: U.S. Geol. Surv. Prof. Paper, v. 550 D, p. D163-171.

Natland, J.H., 1973. Basal ferromanganoan sediments at DSDP Site 183, Aleutian Abyssal Plain, and Site 192, Meiji Guyot, Northwest Pacific, DSDP, Leg 19. *In* Creager, J.S., Scholl, D.W., et al., Initial Reports of the Deep Sea Drilling Project, Volume 19: Washington (U.S. Government Printing Office), p. 629-641.

Peterson, M.N.A. and Goldberg, E.D., 1962. Feldspar distribution in South Pacific pelagic sediments: J. Geophys. Res., v. 67, p. 3477-3492.

Smith, T.V., 1974. Feldspar minerals: Berlin (Springer-Verlag), v. 1, 622 p.

Stewart, R.J., Natland, J.H., and Glassley, W.R., 1973. Petrology of volcanic rocks recovered on DSDP Leg 19 from the North Pacific Ocean and the Bering Sea. *In* Creager, J.S., Scholl, D.W., et al., Initial Reports of the Deep Sea Drilling Project, Volume 19: Washington (U.S. Government Printing Office), p. 615-627.

Weaver, C.E. and Beck, K.C., 1971. Clay water diagenesis during burial: How mud- becomes gneiss: Geol. Soc. Am. Spec. Paper, v. 134, 79pp.

Winterer, E.L., Ewing, J.I., et al., 1973. Initial Reports of the Deep Sea Drilling Project, Volume 17: Washington (U.S. Government Printing Office).

Wright, T.L., 1968. X-ray and optical study of alkali feldspar: II. an X-ray method for determining the composition and structural state from measurement of 28 values from three reflections: Am. Mineral., v. 53, p. 88-104.

Yeats, R.S., Forbes, W.C., Scheidegger, K.F., Heath, G.R., and van Andel, T.H., 1973. Core form Cretaceous basalt, Central Equatorial Pacific, Leg 16, Deep Sea Drilling Project: Geol. Soc. Am. Bull., v. 84, p. 871-882.

PLATE 1

A comparison of textures and mineral preservation in a sequence of volcanogenic sandstone beds from Hole 315A. All bar scales are given in millimeters. All micrographs were taken in plane polarized light.

Figure 1 — 315A-15-2, 44-50 cm (780 m depth). Plain light. Upper Paleocene. Light colored, tan speckled, graded and laminated sand. Components comprise mostly calcareous fossil fragments and dark yellow-brown, rounded palagonite grains. Feldspars (white) are mostly plagioclases and occur both as rare fresh-looking, sub- to euhedral loose individual grains and as laths in glomeroporphyritic clots. Matrix both micrite and clay. Glass and chalcedony present.

Figure 2 — 315A-15-2, 44-50 cm (760 m depth). Plain light. Upper Paleocene. Close-up of a round variolitic aphyric basalt clot and a single vesicle-filling radial zeolite spherulite.

Figure 3 — 315A-20-6, 10-17 cm (830 m depth). Plain light. Upper Campanian. Basal layer of a tan, graded volcanogenic sand. Components are primarily carbonate and palagonite. Feldspars (white grains) are concentrated along the base of the bed. Matrix is clay. Some calcite is present as rare sparry, intergranular cement and as replacement for low birefringent minerals (feldspar?). Most feldspars are plagioclase, but several unaltered alkali-feldspars with gridiron extinction are also present as single grains showing good cleavage.

Figure 4 — 315A-20-6, 10-17 cm (830 m depth). Plain light. Upper Campanian. Close-up of a grouping of fresh-looking, almost euhedral twinned plagioclase grains. Matrix and cement and some micrite. In rare cases grains are bridged by sparry calcite.

Figure 5 — 315A-22-4, 145-150 cm (850 m depth). Plain light. Middle Campanian. Basal portion of thick, greenish-gray, graded and laminated volcanogenic sand layer. Grains are rounded to angular, fresh to completely altered, and supported by a dominantly montmorillonite clay matrix. There is evidence of illitic(?) borders on some grains and fine-grained silica may be present in the matrix. Components are mostly basaltic clots and altered volcanic glass (about 50%), calcareous fragments, and feldspars. Further, components are iddingsite, various zeolites as pseudomorphs, and very rare pyroxene fragments. Most alterations appear to have been in situ without greatly altering the texture. Some calcite grains appear as complete pseudomorphs of feldspars.

Figure 6 — 315A-27-1, 117-120 cm (933 m depth). Transmitted light. Santonian (?). White and tan speckled, laminated volcanogenic siltstone. Laminations have concentrations of red-orange hematite and ilmenite plus plagioclase feldspar laths and various clay pseudomorphs. Dominant clay matrix, light tan to yellowish-green montmorillonite.

Figure 7 — 315-28-3, 50-56 cm (952 m depth). Santonian (?). Light greenish-gray, graded volcanogenic sandstone. Hand specimen exhibits a strong bluish-green cast as solution relict. Grains are mostly subrounded to subhedral twinned feldspars. Both plagioclase and K-feldspar are present. Many sparry calcite pseudomorphs, scattered basalt remnants, and hematite grains are present. Most volcanic glass and mafic components are completely altered to a microcrystalline meshwork of bright blue green and yellow clay, dominantly montmorillonite. Many grains are outlined by a high birefringent mica which also occurs as lacy stringers in the matrix. Matrix and altered volcanic glass have an identical character giving remaining grains a "floating" appearance.

Figure 8 — 315-28-3, 50-56 cm (952 m depth). Santonian (?). Detail of Figure 7 showing disintegration of black altered volcanic glass fragments converting sample to a bluish-green clay montmorillonite.

PLATE 1

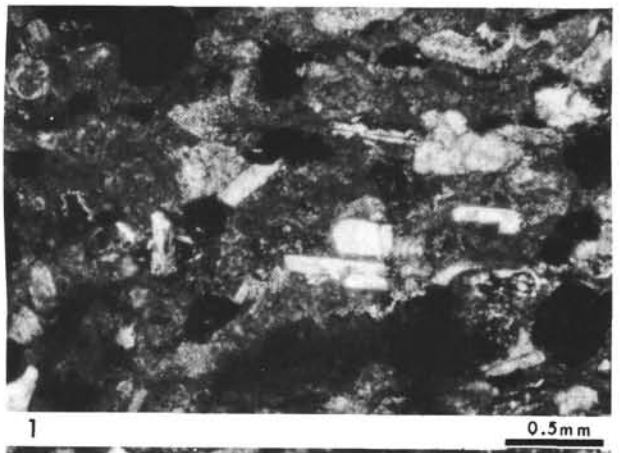

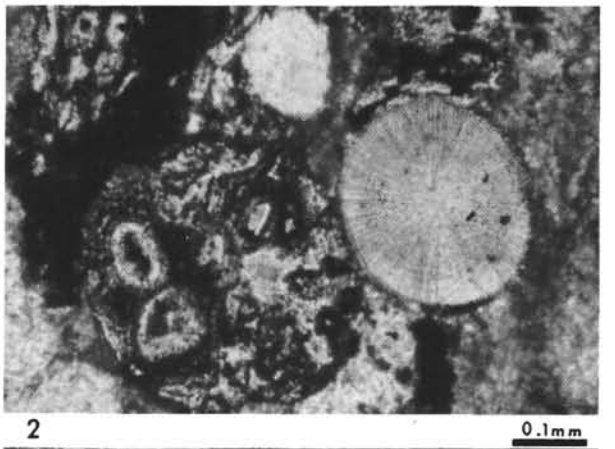

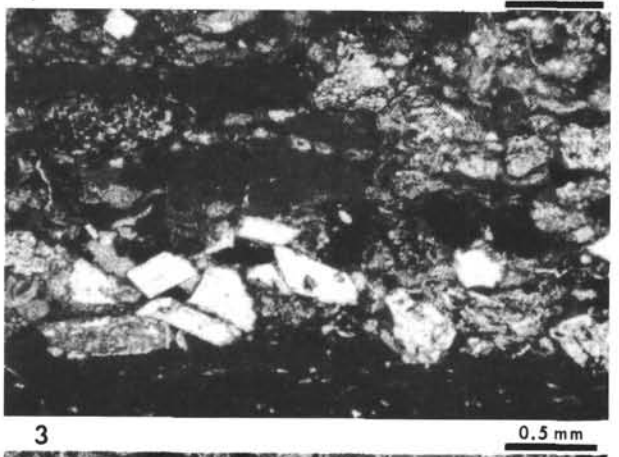

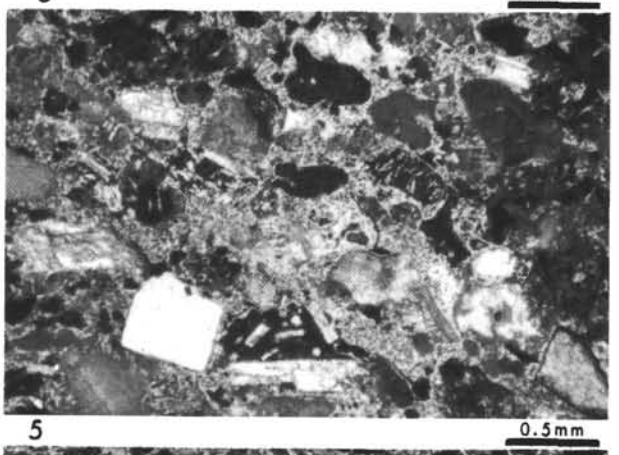

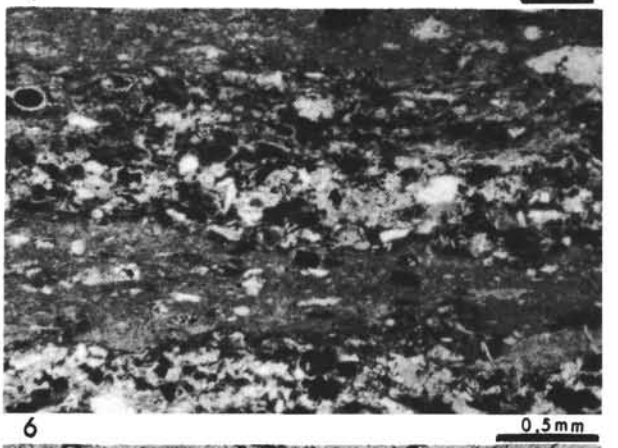

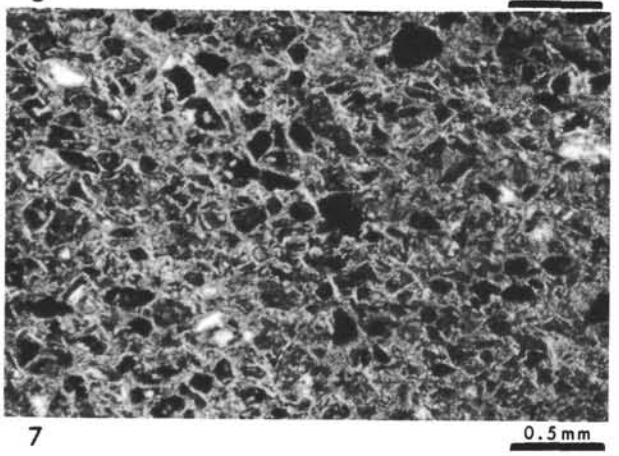

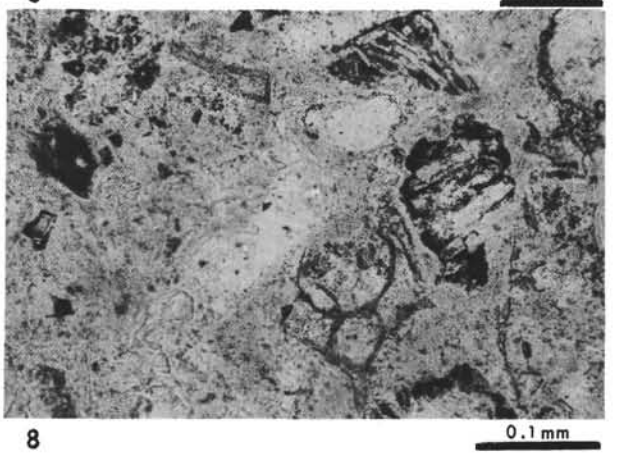

PLATE 2

Hole 315A, Core 22 (850 m depth). Mid Campanian. Sequence of thin sections through a greenish-gray, graded, and laminated volcanogenic unit starting from the base.

Figure 1 — 315A-22-4, 145-150 cm. Oblique reflected light. Bar scale = 1.0 mm. Base part of graded layer. Basal contact not recovered. Moderately well to poorly sorted (0.1-0.6 mm) subrounded to angular components comprising mostly altered variolitic, basaltic glass and altered aphyric basalt clots. Dominant calcite as fossil fragments and micritic grains common. Plagioclase common as tiny laths in basalt grains and as large, single, fresh-looking, broken euhedral grains. Zeolites not common and pseudomorphs common, also rare filling in vesicles and as single grains. Pyroxene fragments are rare. K-feldspars were not positively identified. Matrix is yellowish-green montmorillonite, which may be both transported and/or formed in situ.

Figure 2 — Same as Figure 1; crossed polarizers.

Figure 3 — 315A-22-4, 98-103 cm. Oblique reflected light. Bar scale = 1.0 mm. Grain size decreases to approximately 0.08-0.2 mm grains suspended in a montmorillonite matrix. Fabric lineation is visible. Grains comprise same assemblages as above with exception that single, twinned, plagioclase grains become rare and micritic calcareous components more common. Rounded palagonite grains are more prominent.

Figure 4 — Same as Figure 3; crossed polarizers.

Figure 5 — 315A-22-4, 46-51 cm. Oblique reflected light. Bar scale = 1.0 mm. Upper part of graded layer, light greenish-gray. Well-developed grain-layer fabric. Fine silt grains supported in a clay matrix. Calcite components dominant over palagonite; altered basalt grains and various feldspar fragments commonly occur as sparry calcite. Various zeolite sheaves are present, many as apparently former vesicle fillings.

Figure 6 — Same as Figure 5; crossed polarizers.

Figure 7 — 315A-22-3, 44-49 cm. Plane polarized light. Bar scale = 1.0 mm. Thin section from the brownish-gray topmost, lutitic portion of the graded bed. Burrowing was active in this zone. Recrystallized sparry calcite and cryptocrystalline silica blebs in a mostly micritic and clay matrix. Scattered volcanogenic grains present.

Figure 8 — 315A-22-3, 44-49 cm. Plane polarized light. Bar scale = 0.1 mm. Detail of siliceous blebs containing various inclusions including scattered fine grains of reddish hematite. In rare instances pitting visible along the margins resembling infilling and overgrowths of radiolarian tests. Also, bleb may have grown in situ.

PLATE 2

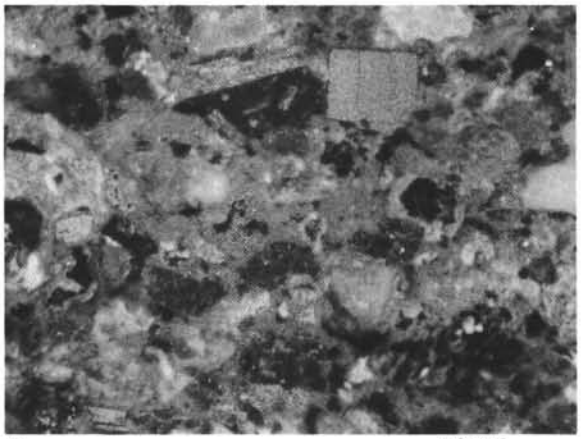

1

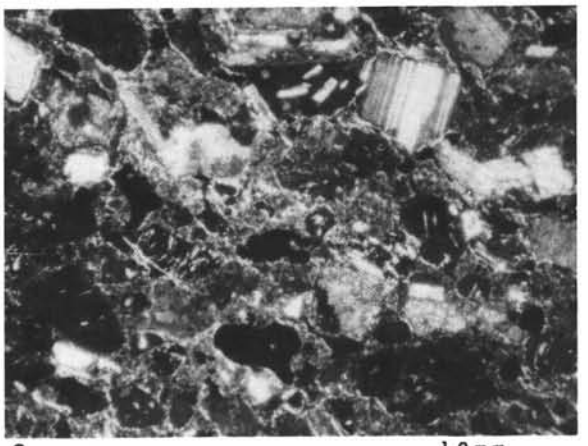

2

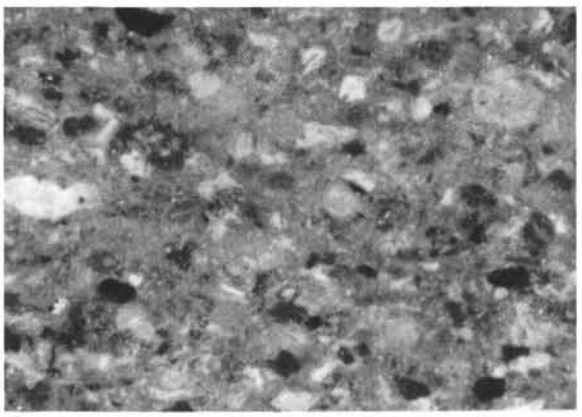

3

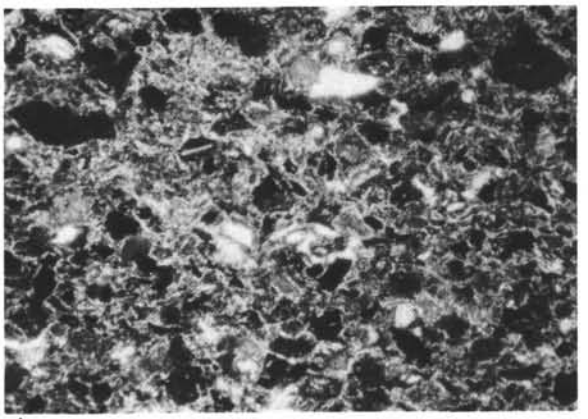

4

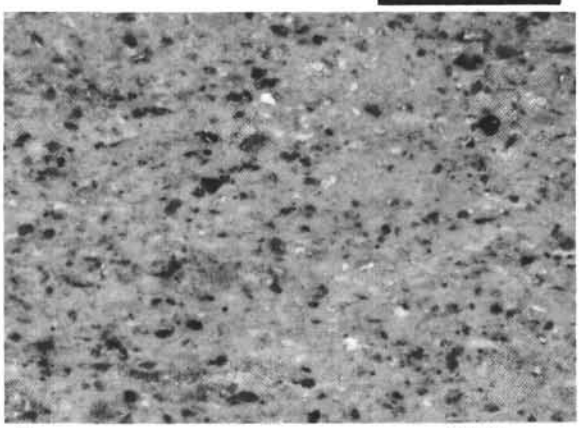

5

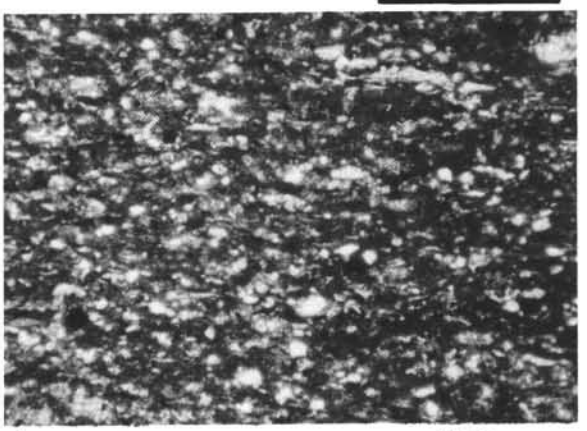

6

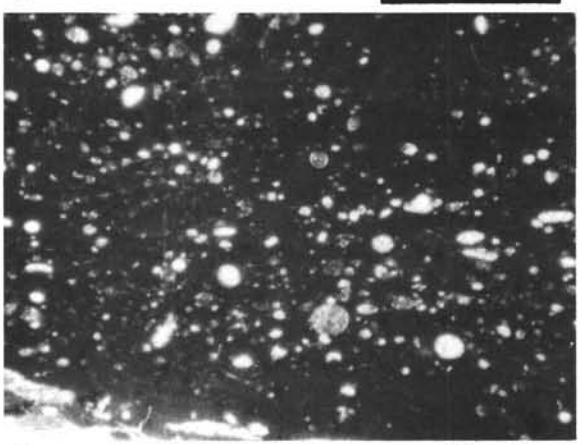

7

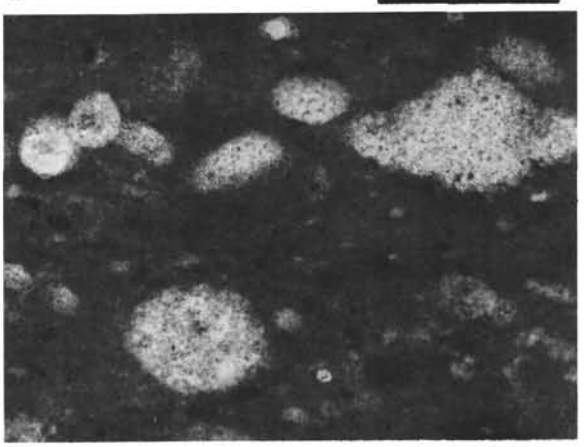

8

PLATE 3

Examples of various modes of occurrence for calcite in basal volcanogenic sediments from Site 316. In slight contrast to Site 315A, calcareous fossil sediments were dominant in the entire 200-meter volcaniclastic section (see Beckman, this volume). Bar scales in millimeters. Dominant (D), Abundant (A), Common (C), Rare (R).

Figure 1 — 315-26-2, 40-42 cm (730 m depth). U. Campanian. Plane polarized light. Sparry calcite cement encompassing altered volcanic glass grain. Twinned K-feldspar in lower left corner. The sample is from a laminated volcanogenic sand, speckled, white tan and reddish. Comprised of abundant rounded volcanic grains including glomeroporphyritic clots, iddingsite and hematite grains, altered glass and rare zeolite bundles, as well as altered plagioclase laths and untwinned feldspar. These grains are mostly highly altered and are set in a sparry calcite mosaic (60%) cement. Scattered micritic grains are present but most fossils have been recrystallized and incorporated into the calcite cement. Some faint outlines persist. Some sparry calcite appears to be pseudomorph after feldspars. Clay totally absent except as rare pseudomorph grains. Therefore, microcrystalline silica may be present in unknown amounts as an alteration product. Much of the alteration and rounding appears to have been in situ. X-ray diffraction suggested the following assemblage: calcite (D), K-feldspar (A), plagioclase (C), and montmorillonite, iron minerals.

Figure 2 — Same as Figure 1; crossed polarizers.

Figures 3-6 — 316-28-1, 138-140 cm (770 m depth). M.-Campanian. From vesicular grains observed in a volcanogenic breccia bed. X-ray diffraction indicates the following bulk mineral composition: calcite (D), montmorillonite (C), K-feldspar (R), analcite (R), and quartz, plagioclase, hematite, and gibbsite. Many of the plagioclase grains have been replaced by analcite and K-feldspar.

3. Plane polarized light. Green, vesicular grain with some patches filled with analcite. Vesicles are ovoid and circular, some lined with radial green zeolite sheaves, then infilled with sparry calcite.

4. Plane polarized light. Altered black scoriaceous basalt fragment. Fine needle-like feldspar laths define a flow fabric. Patches of green clay have formed later. Large elongated pods are filled with sparry calcite. Thin, greenish zeolite linings may be present.

5. Plane polarized light. Large, dark green vesicular clast. Groundmass is a dark green, homogeneous microcrystalline chlorite mass. Vesicles are extremely variable, commonly irregular. Most are lined with clay or zeolite, others filled with single calcite crystals. Analcite may also be present. Feldspars are present as remnant corroded plagioclase laths in the groundmass and as idiomorphic K-feldspar phenocrysts with hollow cores. These apparently have formed around vesicles, and some exhibit faint, zonal structure but no twinning.

6. Plane polarized light. Detail of K-feldspar from above in contact with the groundmass. Step-like edges may be due to primary growth or resorption.

PLATE 3

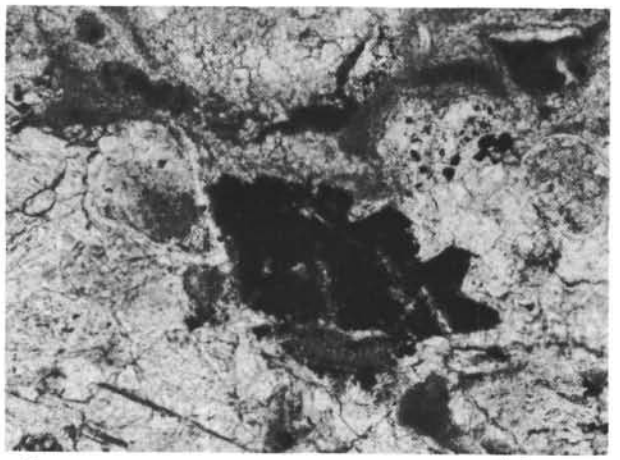

1

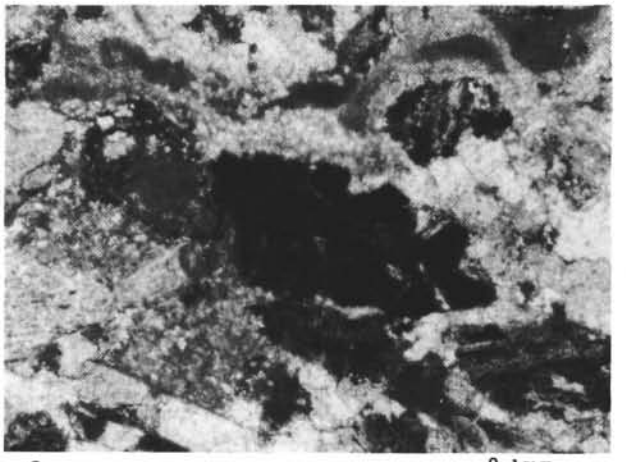

2

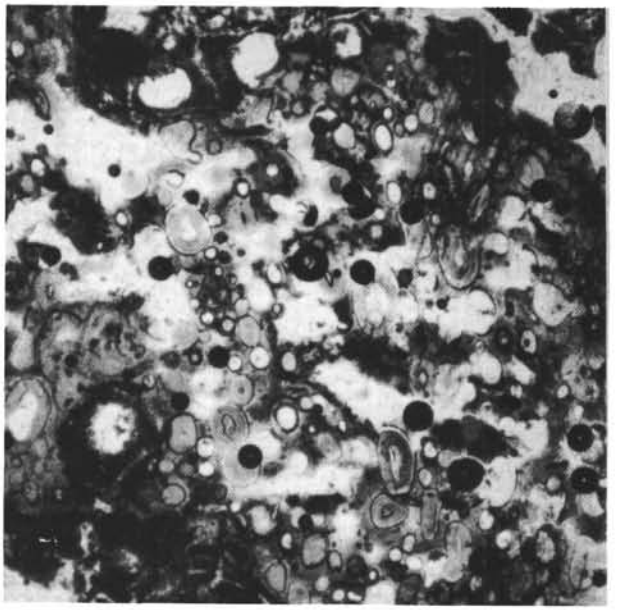

3

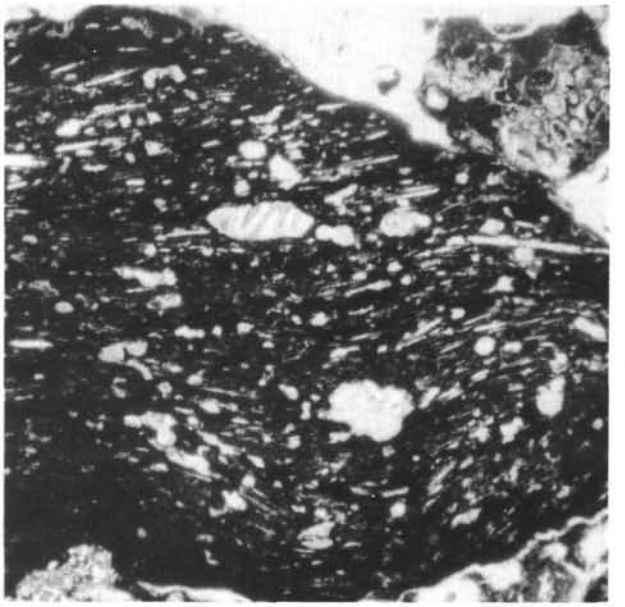

4

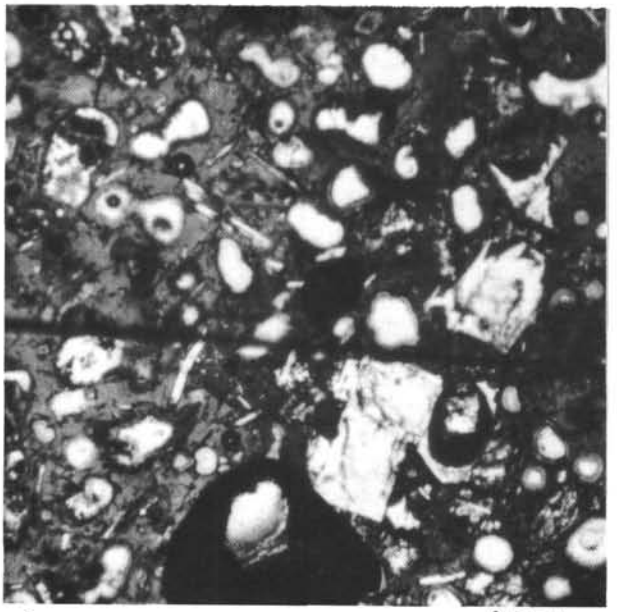

5

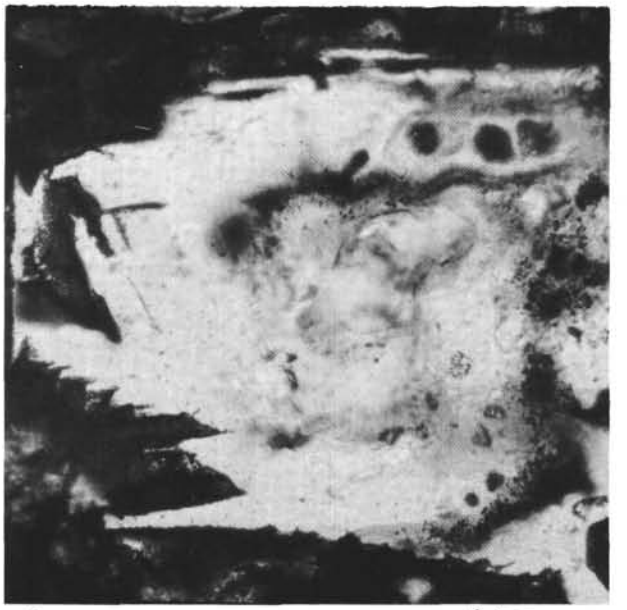

6

PLATE 4

Volcanogenic Sediments

Figure 1 — 315A-30-1, 66-72 cm (985 m depth). Santonian(?). Oblique reflected light. Bar scale = 0.0 mm. Altered vesicular and variolitic angular hyaloclastite shards stand out as light greenish-gray clasts. Dark patches are transparent grains, mostly feldspar, and some zeolites. Montmorillonite clay matrix is light green.

Figure 2 — Plane polarized light. Bar scale = 0.1 mm. Altered hyaloclastic grains, almost opaque. Brown to brownish rims outline clasts. Grains are very poorly sorted with little intergranular space. To the left is an irregular K-feldspar with saw-tooth cavity lining.

Figure 3 — Crossed polarizers. Bar scale = 0.1 mm. Very little clay matrix. Individual grains are separated by a thin border of high birefringent clay, probably illitic. Altered glass consists of a cryptocrystalline dark yellowish-brown montmorillonite mass. Note the homogeneous extinction of the saw-tooth K-feldspars. Centers may be hollow or filled with calcite or rounded altered glass clumps.

Figure 4 — Plane polarized light. Bar scale = 0.1 mm. A glomeroporphyritic clast. Narrow plagioclase laths are altered to K-feldspars. Aphyric groundmass is altered to micro aggregate of montmorillonite clay and iron minerals.

Figure 5 — Plane polarized light. Bar scale = 0.1 mm. A pseudomorph filling of an olivine (?) grain with radial sheaves of yellowish-green zeolite.

Figure 6 — Same as Figure 5, crossed-polarizers. Note high birefringent clay border around grain.

Figure 7 — 315A-28-3, 72 cm (950 m depth). Santonian(?). Bar scale = 0.1 mm. Bright blue-green waxy claystone, which is microscopically homogeneous mixture of high birefringent blue-green montmorillonitic clay and quartz.

Figure 8 — Same as Figure 7; crossed-polarizers.

PLATE 4

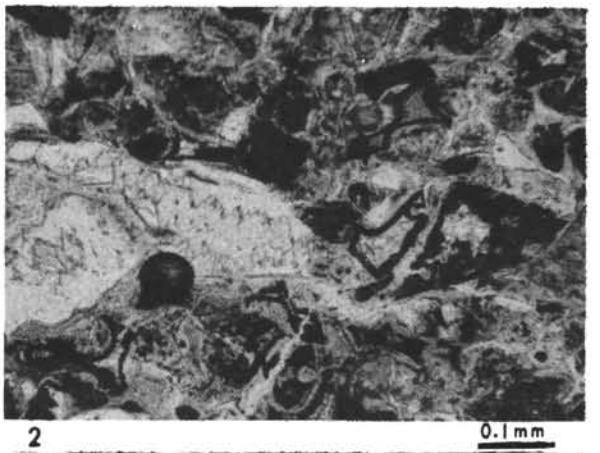

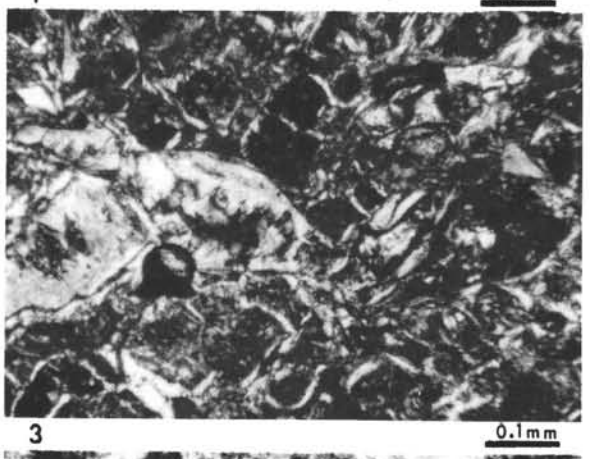

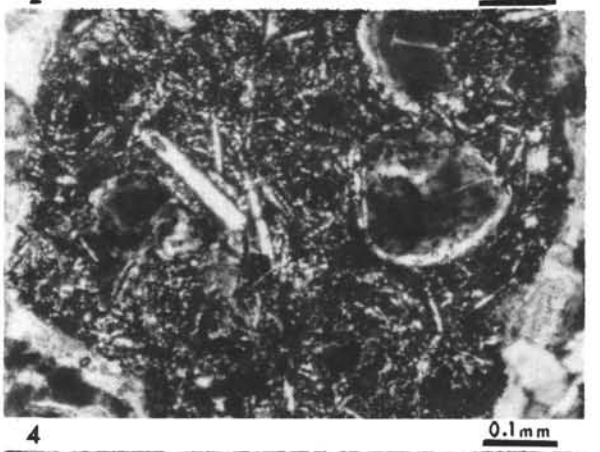

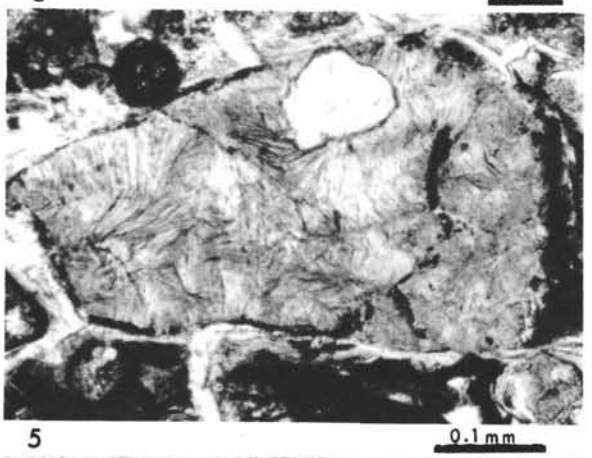

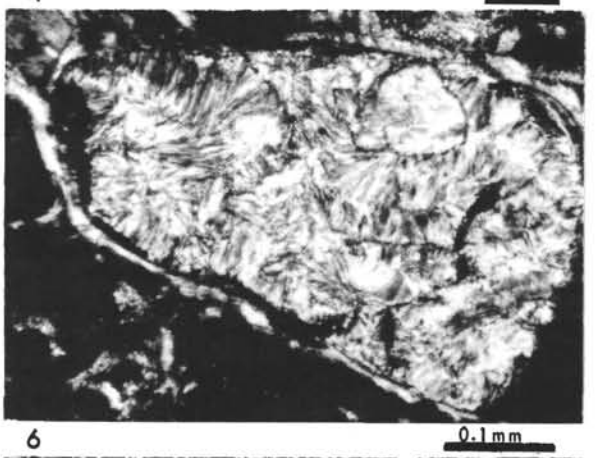

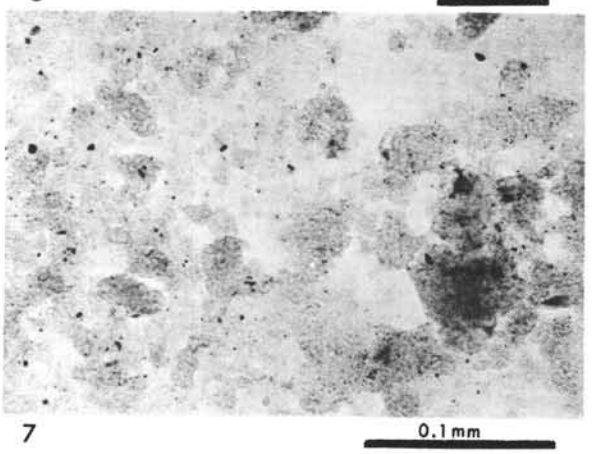

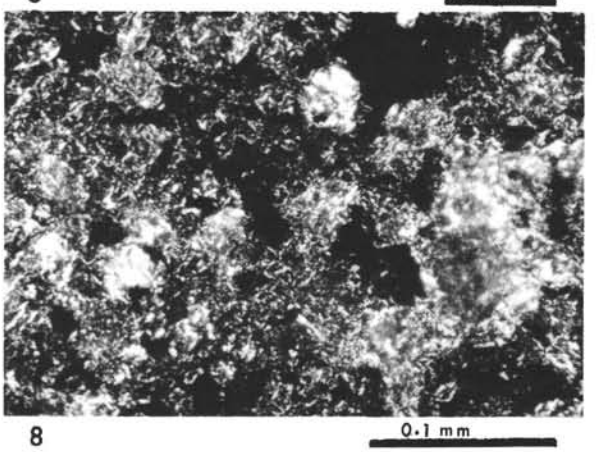

PLATE 5

Various modes of hollow replacement of K-feldspar occurrences. All bar scales = 0.1 mm. Sample 315A-30-1, 66-71 cm (985 m depth). Santonian

Figure 1 — Plane polarized light. Rounded replacement K-feldspar grain with high reflective index inclusions in patches which are oriented along parallel crystallographic planes.

Figure 2 — Same as Figure 1; crossed-polarizers. Homogeneous extinction, no cleavage.

Figure 3 — Plane polarized light. Subhedral replacement K-feldspar with saw-tooth cavity lining.

Figure 4 — Same as Figure 3; crossed-polarizers.

Figure 5 — Plane polarized light. Nearly euhedral replacement K-feldspar with almost complete stepwise idiomorphic infilling. Spherical inclusion is a dark brown altered basaltic glass aggregate set in an isotropic background.

Figure 6 — Same as Figure 5; crossed-polarizers.

Figure 7 — Detail from Figure 1, plane polarized light oriented apatite(?) inclusions.

Figure 8 — Plane polarized light. Rounded to subhedral replacement forms with inner cavity filled with sparry calcite.

PLATE 5

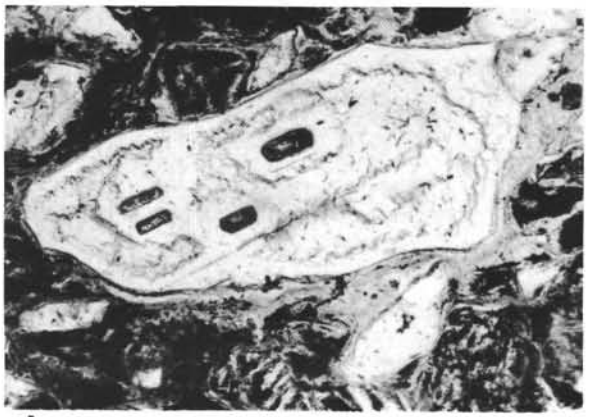

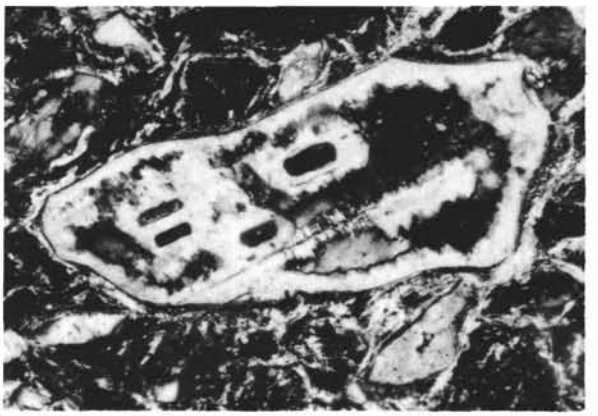

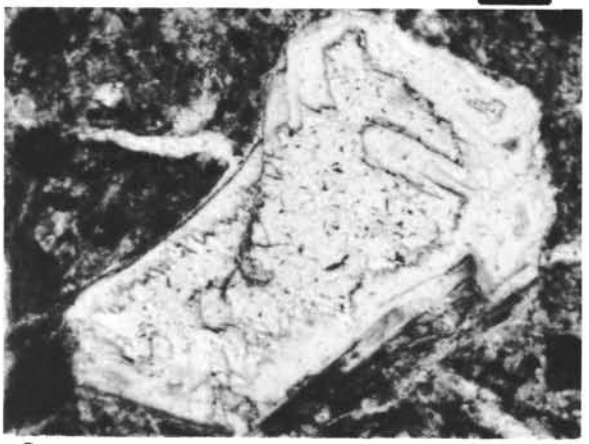

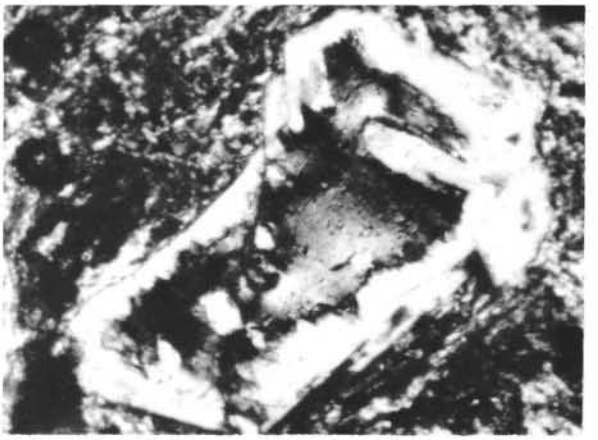

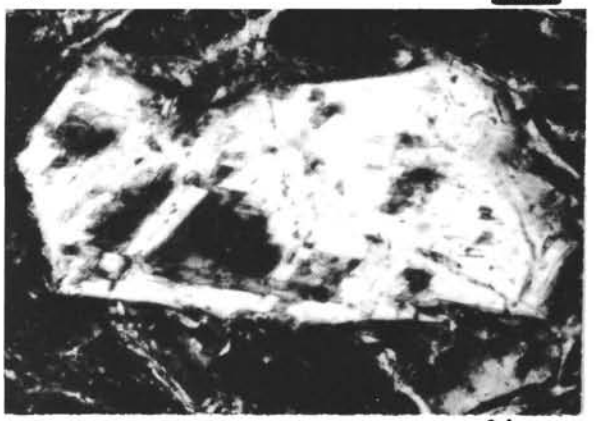

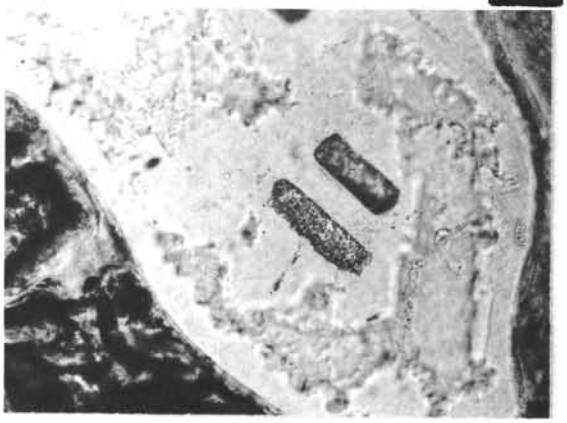

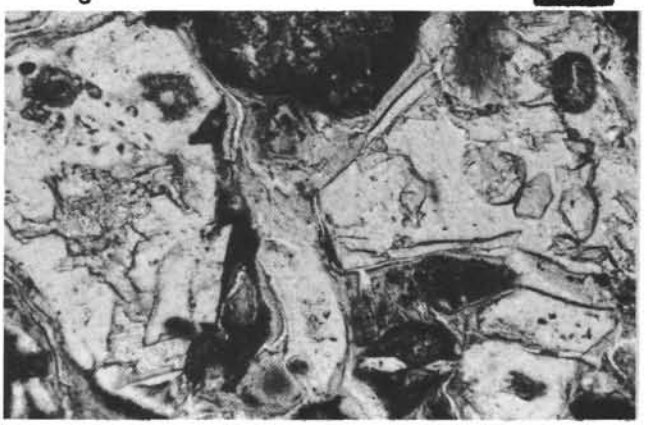

PLATE 6

Scanning electron micrographs of the ultramorphology of cavity linings from replacement K-feldspar (intermediate microcline). Sample 315A-29-2, 22-26 cm (970 m depth), Santonian(?).

Figure 1 — Bar scale = 100μm. Overview of a hollow replacement K-feldspar grain (compare with Plate 5). Outer homogeneous K-feldspar rim is thin, lined with blocky idiomorphic prisms. Solution or resorption textures are not visible. Numerous inclusions are perched along the cavity lining, probably they are alteration products of altered basaltic glass inclusions. Optically phyllosilicate inclusions are greenish whereas K-feldspar is clear, almost transparent. The exterior of the grain appears fresh with slight pitting and only slight patchy clay growth.

Figure 2 — Same as Figure 1. Bar scale = 20μm. Close-up of features along the lower part of the K-feldspar cavity. Note in the center of the SEM micrograph leafy blades growing from the edge of a stubby striated prismatic grain. EDAX readings on the blocky crystal showed only the presence of Al with some Fe and K, without Si, whereas bladed sheaves registered only Al and Fe again without Si. This could suggest dickite and/or gibbsite. Well-developed euhedral K-feldspar crystal growth as part of the lining has been tentatively assigned crystallographic indexes (courtesy of Dr. H.U. Nissen). EDAX readings show only Si, Al, and K.

Figure 3 — Same as Figure 1. Bar scale = 2 μm. Ultramorphology of unknown (Al/Fe) inclusion mineral. Note the partings and splitting of the 0.5μm thick blades. Wedge-shaped, large blocky blades might be a low Si zeolite or gibbsite.

Figure 4 — Bar scale = 10 μm. Ultramorphology of alteration products lining the cavity of another replacement K-feldspar grain. EDAX analysis of blocky prisms show (in order of peak intensity) Si, Al, K, and a slight trace of Fe; indicates pure K-feldspar. The idiomorphic assemblage in the cavity is greenish and shows Si, Fe, Al, K, and Mg suggesting chlorite and mica. Note the numerous idiomorphic crystals in the leafy aggregates.

PLATE 6

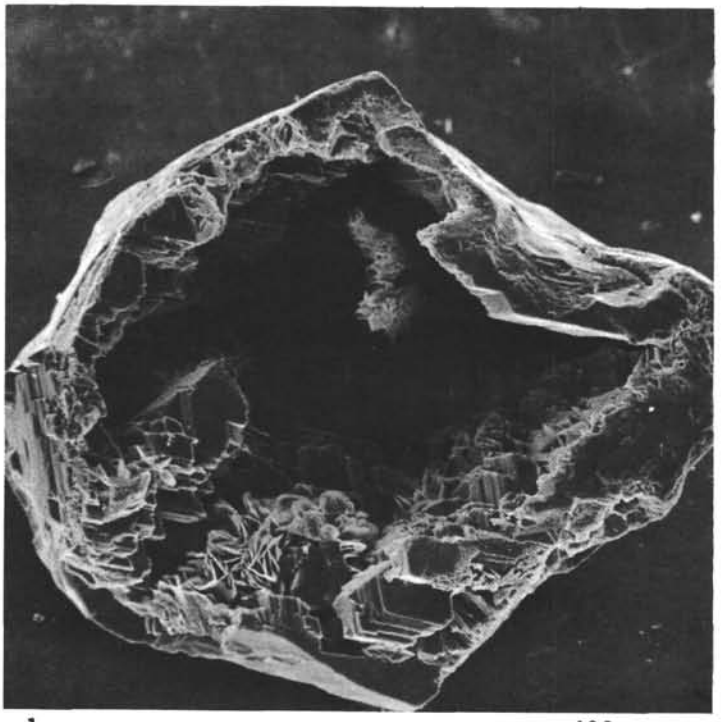

1

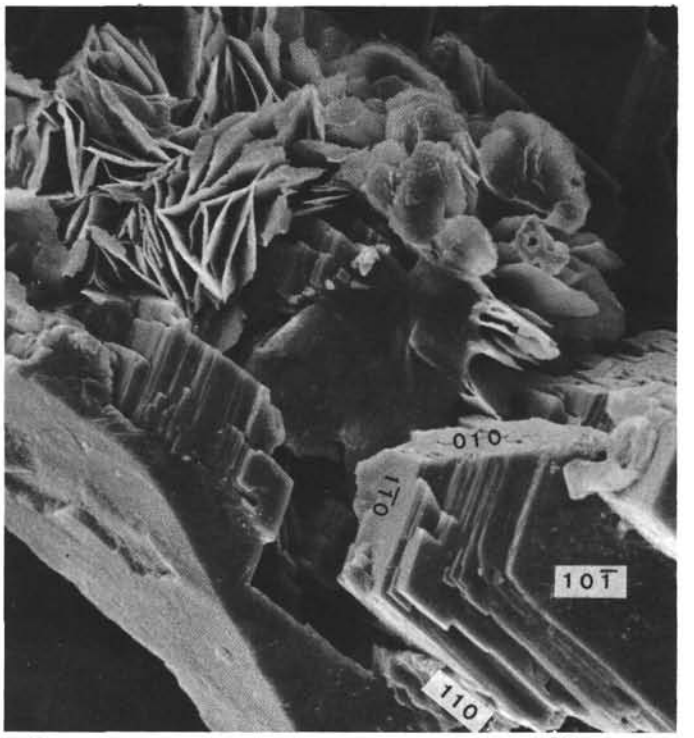

2

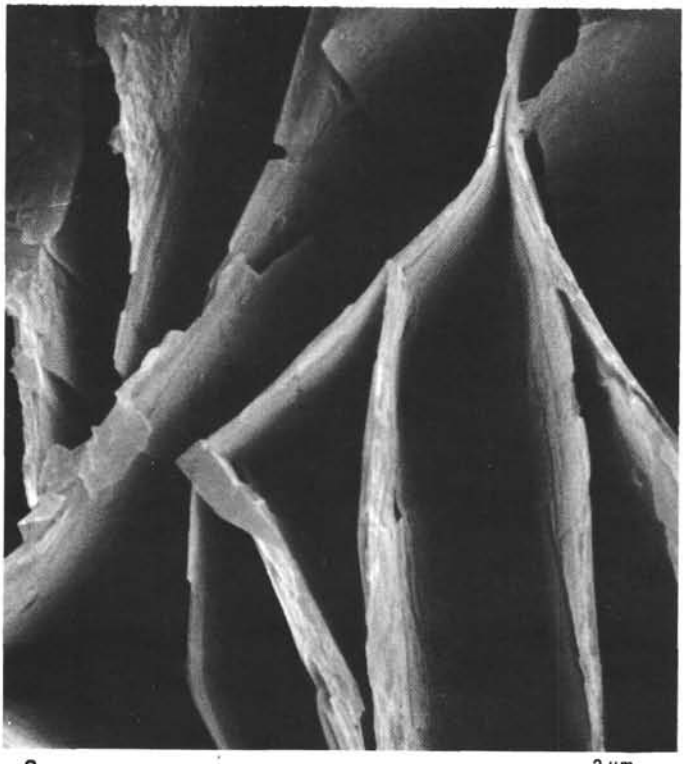

3

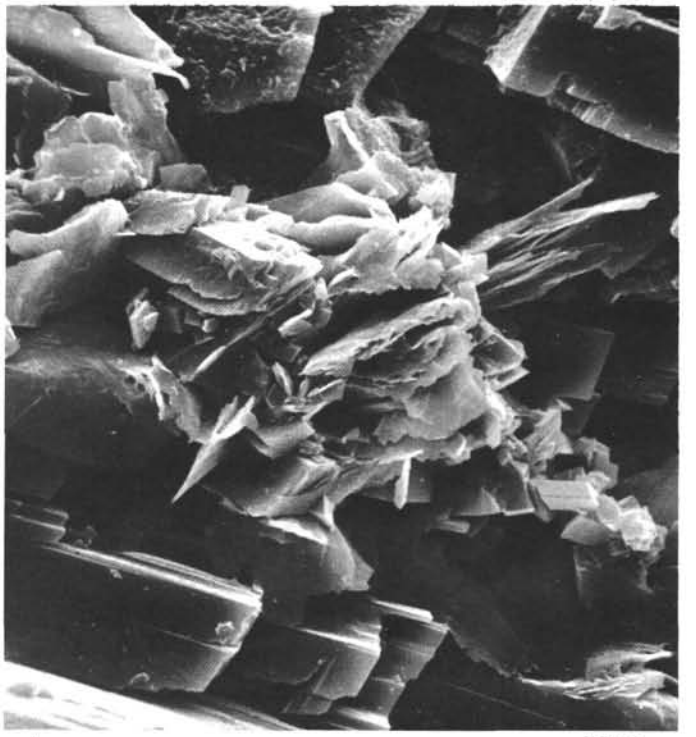

4

PLATE 7

Figure 1 — 315A-30-2, 92-94 cm (990 m depth). Plane polarized light. Santonian(?). Bar scale = 0.5 mm. Thin section showing K-feldspars which was identified as anorthoclase from the first greenish-black volcanogenic graded unit overlying the basaltic basement. In this sample no hollow K-feldspars were observed. Most are subhedral and some exhibit irregular Carlsbad-type twinning. Many varied inclusions of altered volcanic glass and clay are commonly oriented along crystallographic planes. Extinction is irregular and patchy, commonly under higher magnification visible as a Moire gridiron pattern. Similar grains were not observed above Core 30.

Figure 2 — Same as Figure 1; crossed-polarizers.

Figure 3 — Same as Figure 1. Bar scale = 0.1 mm. Close-up of irregularly twinned grained. Note state of alteration and subparallel orientation of inclusions.

Figure 4 — Same as Figure 3; crossed polarizers. Gridiron meshwork submicroscopic twinning together with irregular Carlsbad (Maneback) Lamellae.

Figure 5 — 315A-30-1, 66-72 cm (985 m depth). Santonian(?). Bar scale = 0.1 mm. Dark greenish-gray volcanogenic sand. Detail of a K-feldspar replacing another feldspar(?) phase. Irregular patches of altered hyaloclastic glass occur as patches along twin lamellae. Grain has a border of high birefringent (illite?) mica. In places K-feldspar replacement appears to engulf matrix components.

PLATE 7

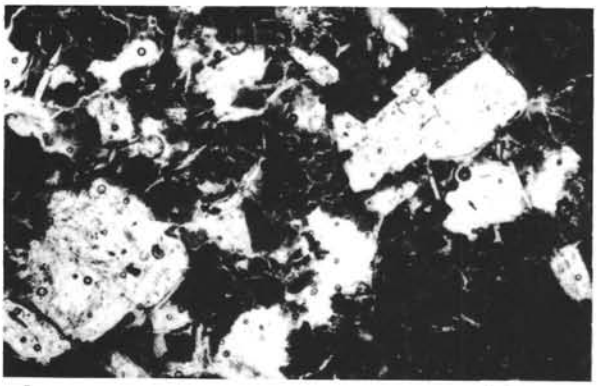

1 0.5mm

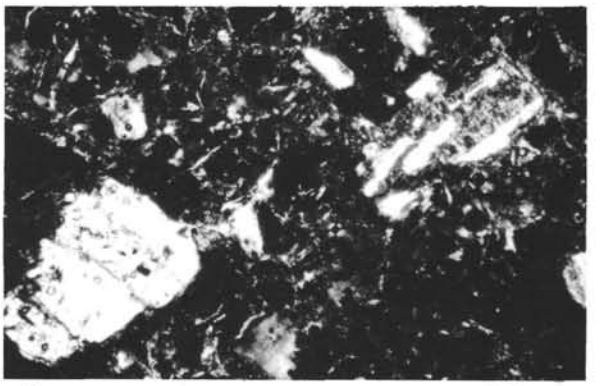

2 0.5mm

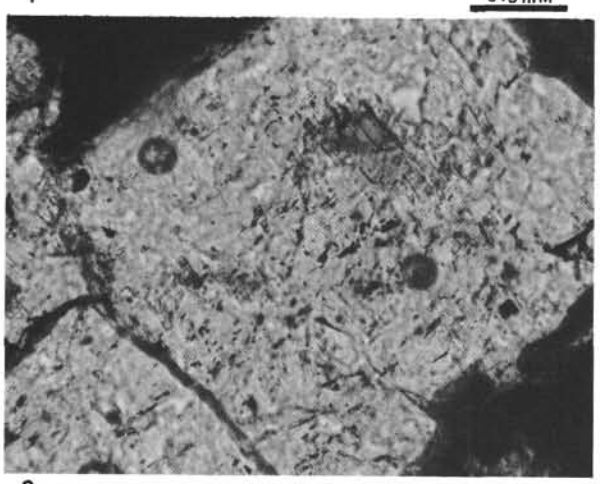

3 0.1mm

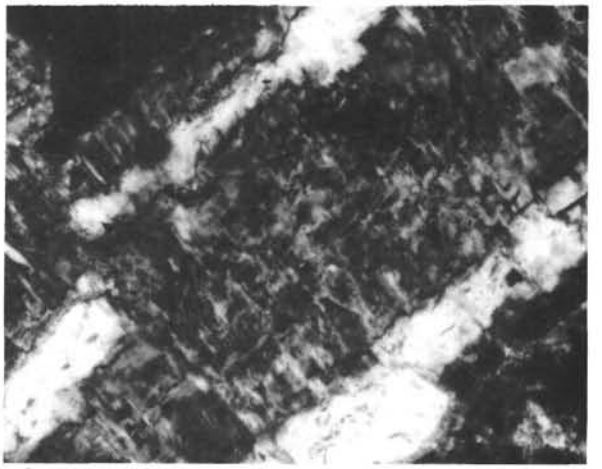

4 0.1mm

5 0.1mm

PLATE 8

Hyaloclastic textures and variolitic volcanogenic sands.

Figure 1 — 315A-30-2, 92-94 cm (990 m depth). Santonian(?). Oblique reflected light. Bar scale = 0.5 mm. Subrounded and angular, variolitic hyaloclastic grains are visible as white. Aphyric basaltic clots are interspersed. Intergranular space is small and clay filled. Extensive in situ alteration of components to clay aggregates.

Figure 2 — Same as Figure 1. Plane polarized light. Light areas consist mostly of K-feldspar, anorthoclase, and orthoclase. Calcite cement or filling is absent.

Figure 3 — 315A-30-1, 66-72 cm (980 m depth). Santonian(?). Plane polarized light. Bar scale = 0.5 mm. Similar to Figure 2. Hyaloclastite clasts outlined by a light yellow-brown altered glass (montmorillonite) rim. Interior with transparent, light greenish sheaves (chlorite?). Intergranular clay matrix is more conspicuous than above. Calcite present as rare grain replacements.

Figure 4 — Same as Figure 3; crossed polarizers. Note how clasts are set in a mosaic of high birefringent clays (illite).

Figure 5 — Same as Figure 4. Oblique reflected light. Texture of very irregular and angular altered hyaloclastic grains in a montmorillonite matrix.

Figure 6 — 315A-29-1, 40-44 cm (950 m depth). Santonian(?). Oblique reflected light. Bar scale = 0.1 mm. Volcanogenic clast comprised (0.1 mm) of spherical vesicles. Most have a clay aggregate lining without zeolites or calcite. (Compare with Plate 10.)

Figure 7 — 315A-30-1, 66-72 cm (980 m depth). Santonian(?). Oblique reflected light. Bar scale = 0.0 mm. Vesicular clast, some vesicles filled with high birefringent clays. Others with a thin clay lining. Highly altered glass. (Compare with Plate 10.)

PLATE 8

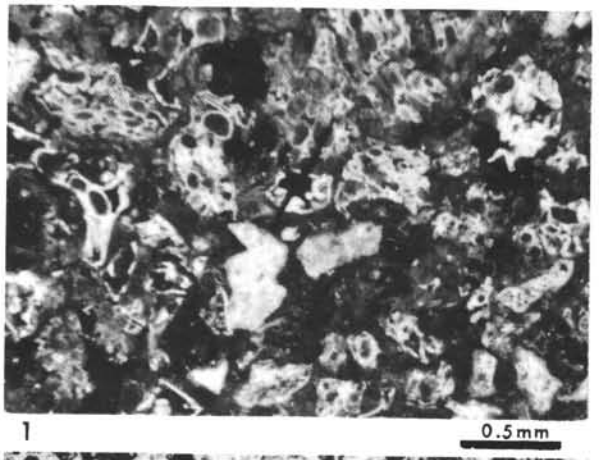

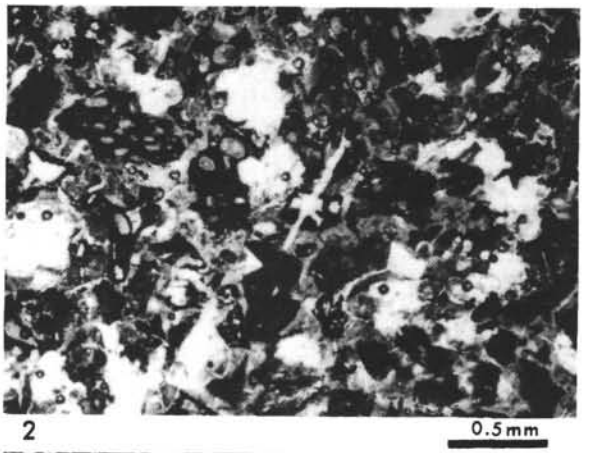

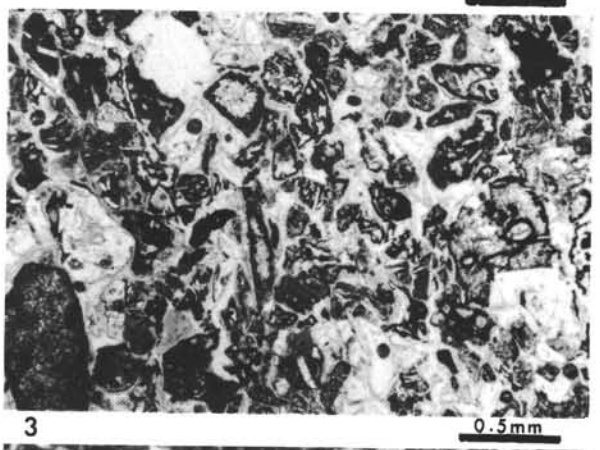

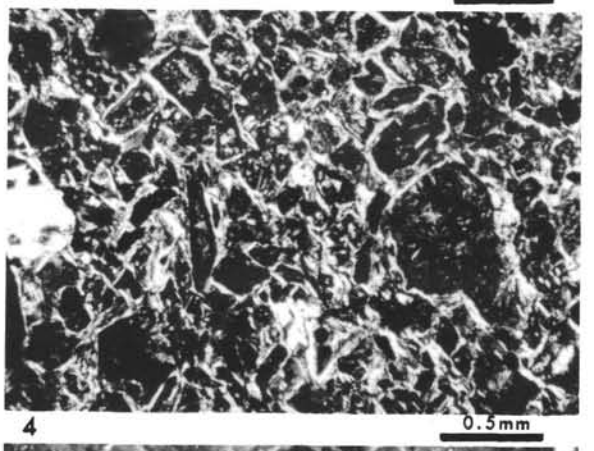

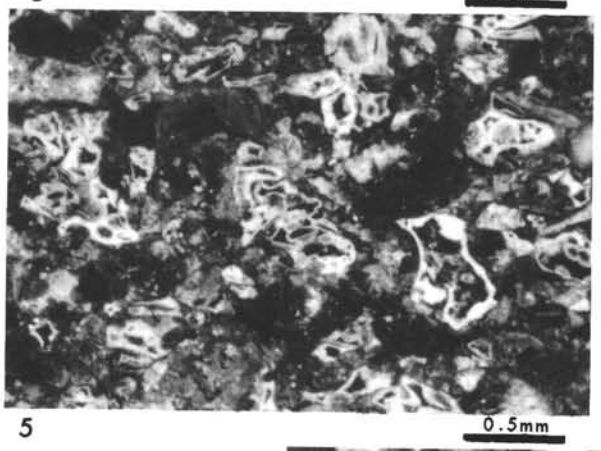

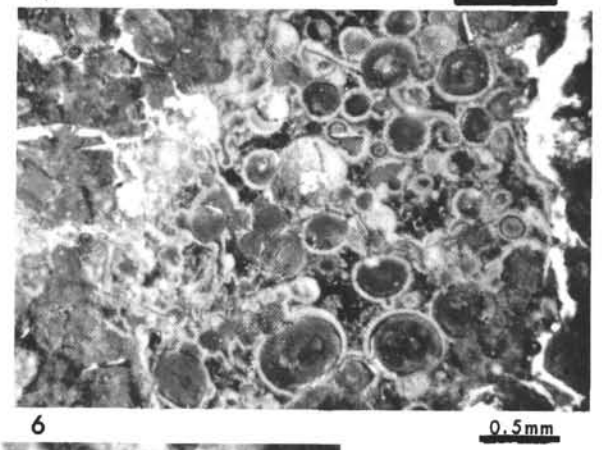

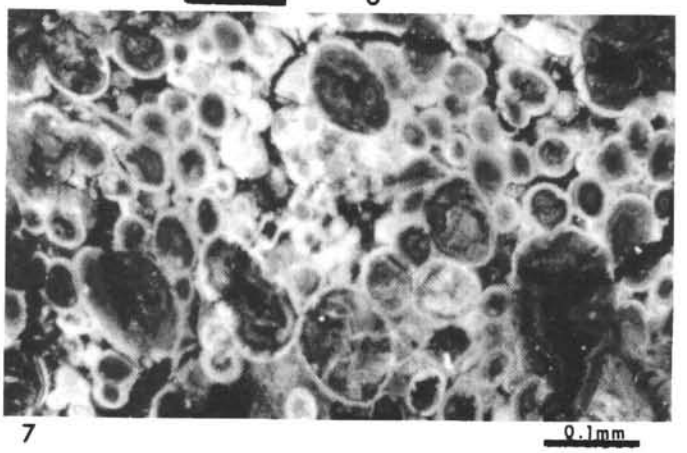

PLATE 9

Scanning electron micrographs.
Alteration/morphology of volcanic shards.

Figure 1 — 315A-29-1, 43-44 cm (970 m depth). Santonian(?). Bar scale = 100 μm. Vesicular clast (compare Plate 8, Figure 6) from dark greenish-gray volcanogenic sand. Fragments separated by dry sieving. Greenish-gray, angular grains. Overview of glass fragments showing spalling effect. One variole is filled and two are simply shells. Note the radial crown around the varioles and the bladed mineral texture of the matrix or groundmass which is light green in optical investigations. EDAX analysis shows the altered glass center filling to consist of Si, Fe, Al, K, Ti, and Mg in order of peak intensity. The crown comprises Si, Fe, Al, Mg, K, and Ti whereas the Fe content and Mg are distinctly higher than the core filling. The leafy matrix is Si, Fe, Mg, K, Al, similar to the crown; however, K and Al are distinctly less, and Ti was not registered. This suggests that the sheaves are probably chlorite and the vesicles may also have a rim with illite or illite/chlorite mixture.

Figure 2 — Same as Figure 1. Bar scale = 5 μm. Morphology of radial sheaves of phyllosilicate, chlorite(?), from the altered glass groundmass.

Figure 3 — Same as Figure 1. Bar scale = 10 μm. Morphology of illite/chlorite(?) crown surrounding an unfilled vesicle.

Figure 4 — Same as Figure 1. Bar scale = 1 μm. Ultramorphology of matrix-filling phyllosilicate sheaves. Note the smooth wafer-thin texture of blades peeling off other sheaves. Extremely high surface area ratios result from such open structures.

Figure 5 — Same as Figure 1. Bar scale = 0.5 μm. Ultramorphology along inside lining of an unfilled vesicle. Lift-up growth of tiny montmorillonite blades. Vesicle wall appears as thin, relatively impervious monomineralic lining, probably restricting infilling.

Figure 6 — 315A-29-1, 44-46 cm (970 m depth). Santonian(?). Bar scale = 2 μm. Another devitrified variolitic volcanic glass grain. Radial arrangement of phyllosilicate sheaves may be a result of primary spalling textures. Surface of the grain shows a coating of irregular montmorillonite.

PLATE 9

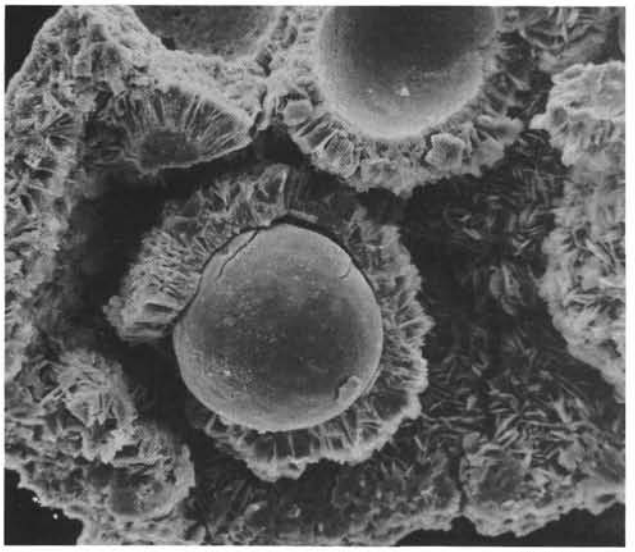

1

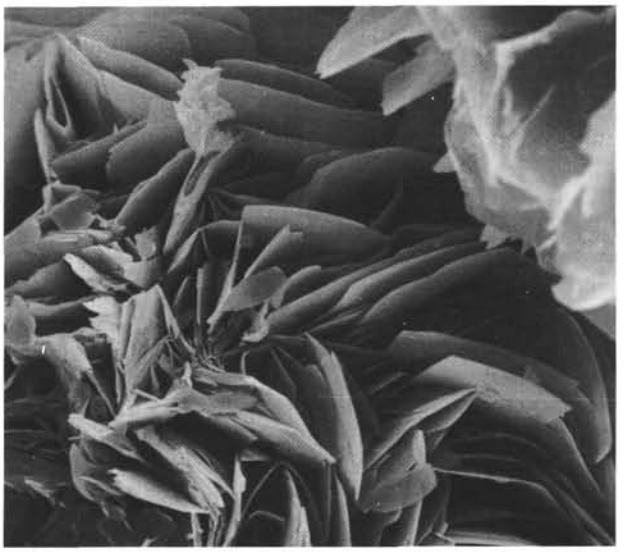

2

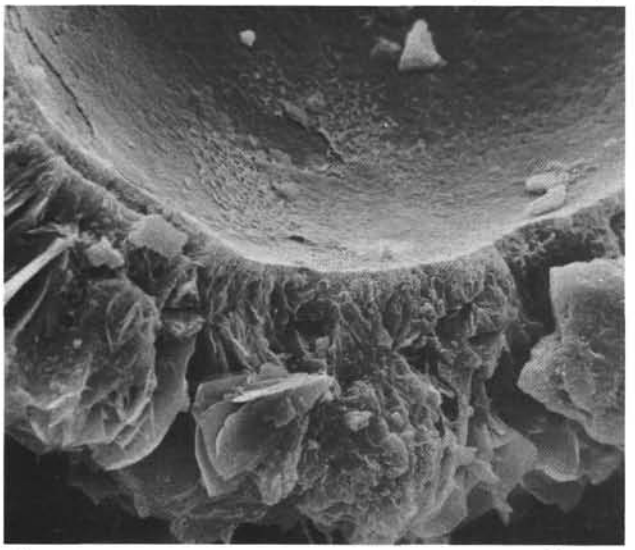

3

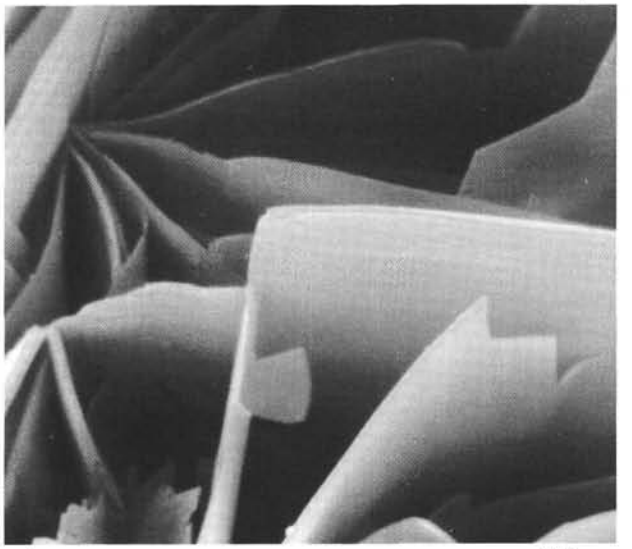

4

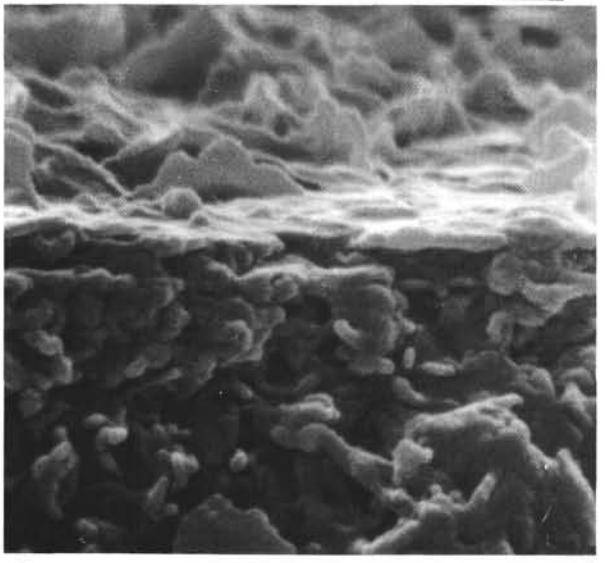

5

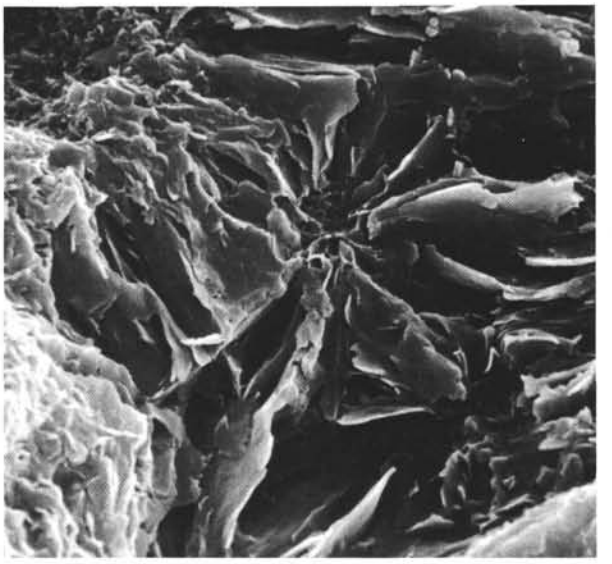

6

PLATE 10

Surface ultramorphology of a potash feldspar grain.

Figure 1 — 315A-29-1, 43-44 cm. (970 m depth). Santonian(?). Bar scale = 100μm. Gives an overview of an idiomorphic broken K-feldspar grain. Optically it is colorless and transparent. Minor twin visible on the surface. EDAX analysis on the clean crystal face revealed a composition of Si, Al, K, a trace of Fe, suggesting a pure K-feldspar.

Figure 2 — Same as Figure 1. Bar scale = 10 μm. Close-up of the center of the feldspar grain. Leaching and alteration of the silicate framework along well-defined lattice planes.

Figure 3 — Same as Figure 1. Bar scale = 2 μm. Detail of the alteration along lattice planes. An intertwinned network of possible remnant crystal framework and clay mineral growth is visible. Tiny blebs on the surface (0.2 μm) may be amorphous allophane or iron oxide.

Figure 4 — Same as Figure 1. Bar scale = 1 μm. Ultramorphology of the skeleton-like interior alteration structures. Spanning the framework voids. EDAX analysis revealed a composition of Si, Fe, Al, K, and a trace of Ca. This is similar to the feldspar crystal except a large increase in K and Fe, suggesting a possible mica phase, so-called potassium smectite or mixed-layered clay. The bulbous appearance of the blade edges may be due to growth texture, bacterial action, or iron-oxide coating.

Figure 5 — 315A-29-1, 43-44 cm (970 m depth). Santonian(?). Bar scale = 20 μm. Fragment of altered volcanogenic glass. Broken surface reveals a thick montmorillonite outer mantle whereas the interior has the texture of spalling variolitic glass. Inward alteration by diffusion apparently proceeds very slowly.

PLATE 10

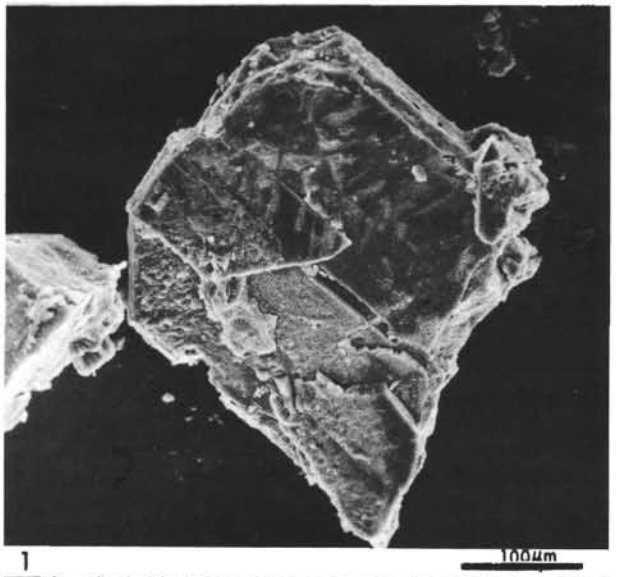

1

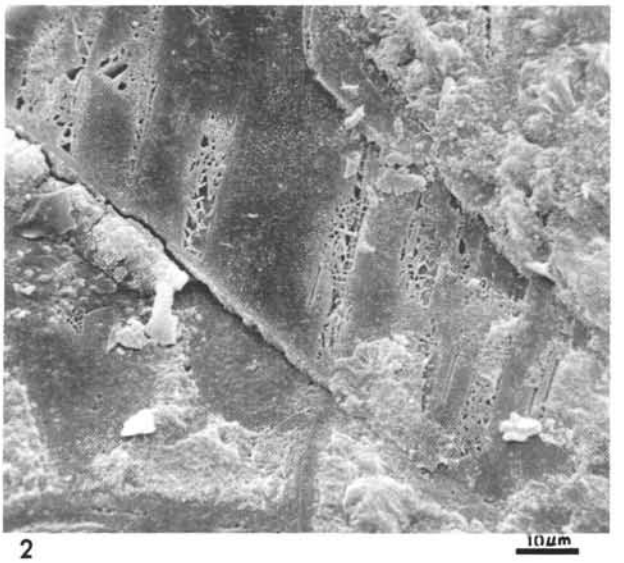

2

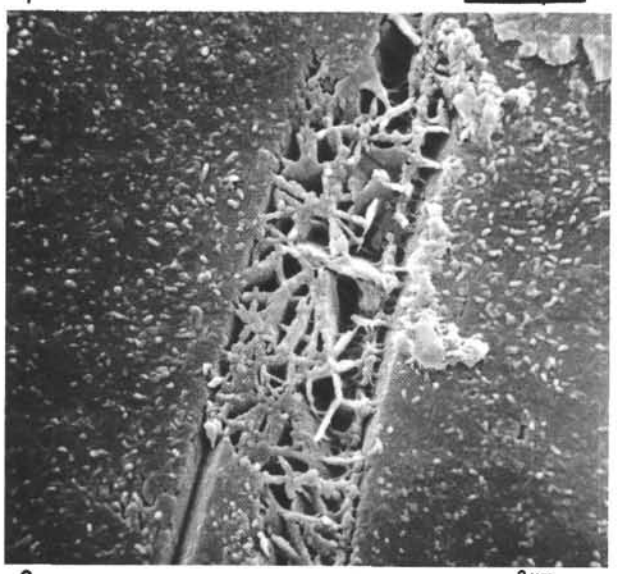

3

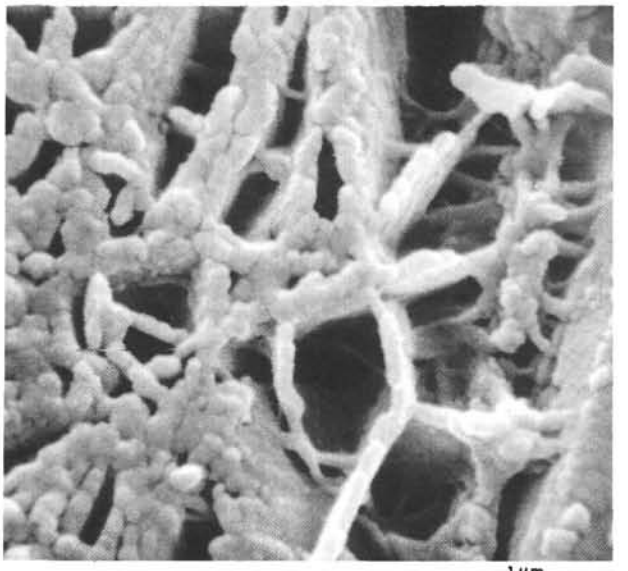

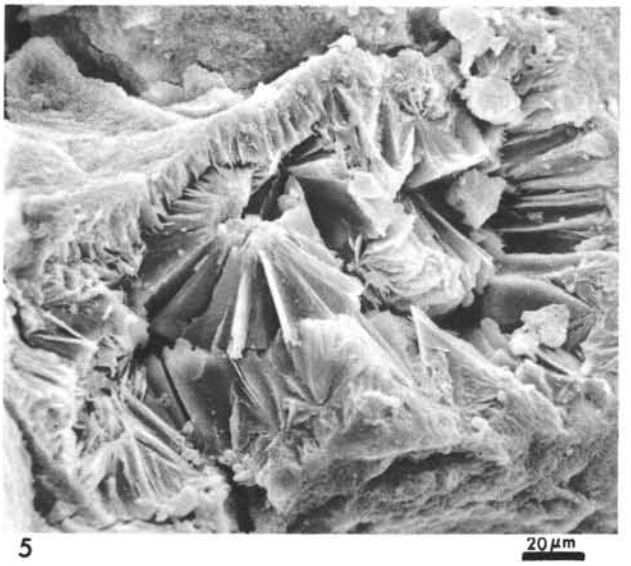

5

PLATE 11

Scanning electron micrographs of pure K-feldspar.
Surface morphology and alteration products.
Sample 315A-29-2, 22-26 cm (970 m depth). Santonian(?).

Figure 1 — Bar scale = 10 μm. Overview of a nearly euhedral part of a K-feldspar crystal. Note that the surface shows three special features of interest: on the left, a crystal face with both preferentially oriented dissolution features and patchy growth of clay colonies, and, on the right, a solution pit etched into the crystal surface. These are examined below under higher magnification.

Figure 2 — Same as Figure 1. Bar scale = 1 μm. Stage 2 alteration. Poorly formed clays grow on surfaces of leached pits in the feldspar crystal. Can be simultaneous with Stage 1. It is not certain whether the clays are a direct product of the solution of the feldspar grain or precipitated from general pore solutions.

Figure 3 — Same as Figure 1. Bar scale = 1 μm. Surface of the feldspar is covered by an almost monomineralic layer of clay. Seen in the thin sections as a thin zone with very high birefringence. May be a mixed-layer montmorillonite/mica, or illite. EDAX indicates K-rich.

Figure 4 — Same as Figure 1. Bar scale = 1 μm. Stage 1; solution features on the feldspar surface. The slightly matty appearance may be due to the presence of an ultra-thin coat of amorphous iron oxide. However, the orientation of the dissolution features along certain lattice planes is evident. These are similar to patterns obtained by the artificial etching of some feldspar with HF acid. Compositions confirmed by EDAX analysis of Si/Al/K-Fe.

PLATE 11

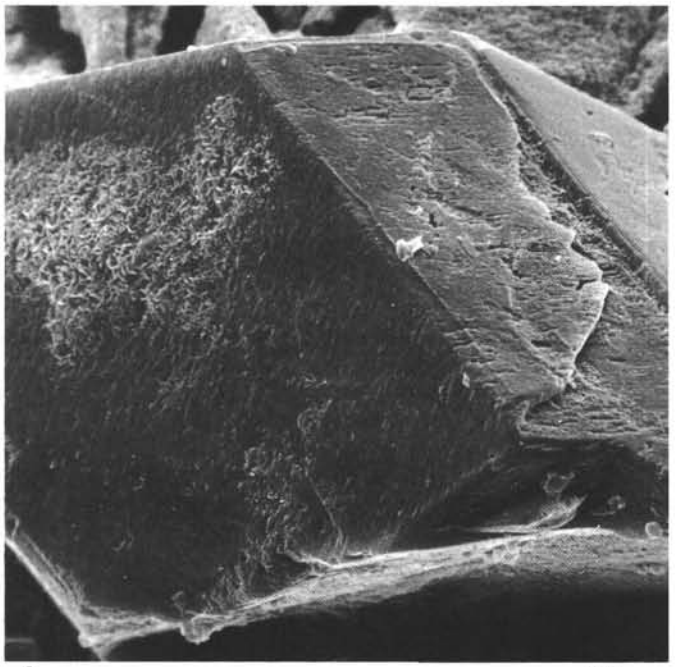

1

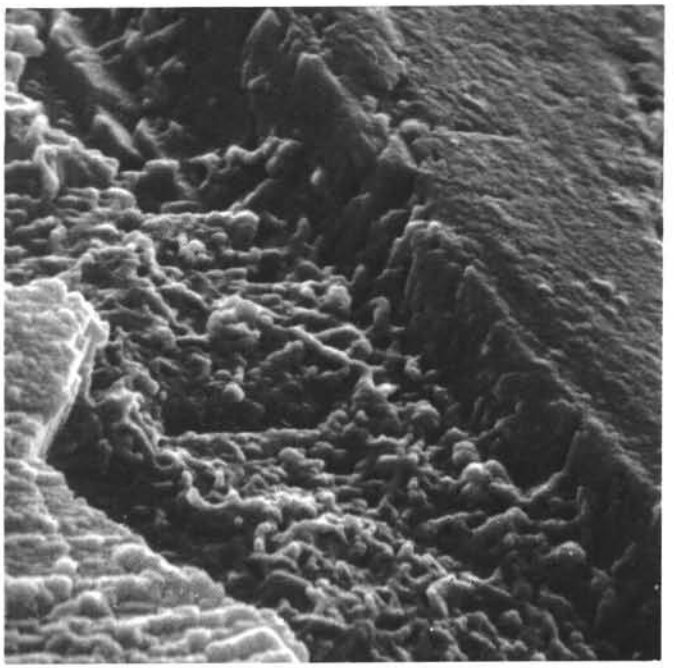

2

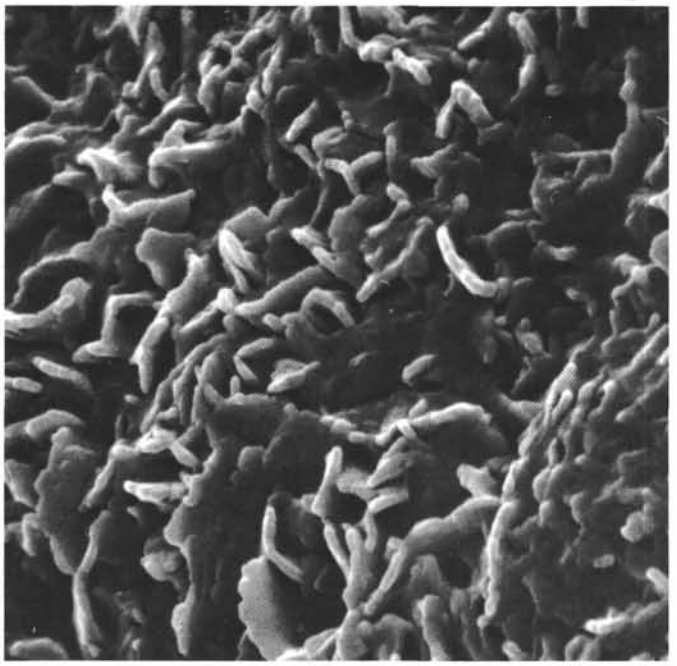

3

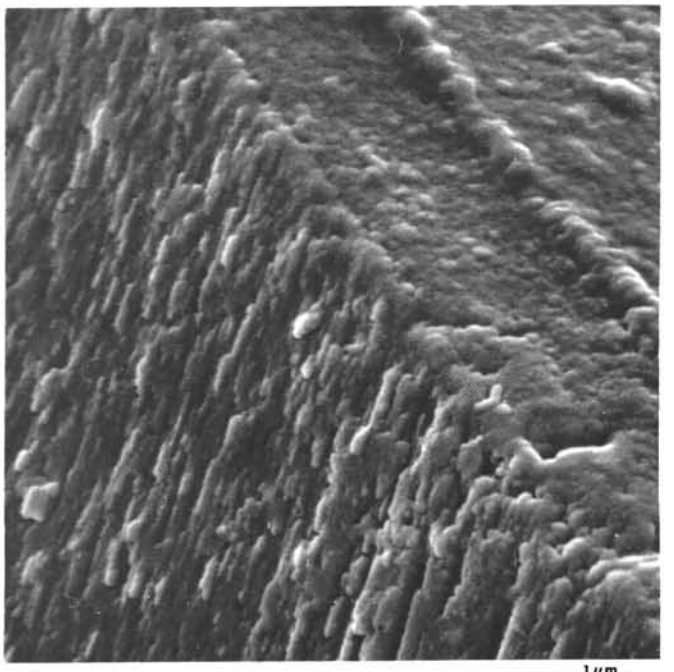

4

PLATE 12

Scanning electron micrograph of pure K-feldspar grains. Surface morphology and alteration. Sample 315A-29-2, 22-26 cm (970 m depth). Santonian(?).

Figure 1 — Bar scale = 100 μm. Overview of almost euhedral K-feldspar grain. A small amount of altered, vesicular, green basaltic glass is adhering to the center part of crystal. EDAX analysis on the upper, clean surface of the grain confirms the K-feldspar composition with a strong pattern of Si/Al/K and a trace of Fe, probably as iron oxide surface contamination. EDAX readings on the altered vesicular material show Si + Fe/K, Al, Mg, and a trace of Na as a probable montmorillonite/mica or chlorite phase.

Figure 2 — Same as Figure 1. Bar scale = 10 μm. Close-up of the K-feldspar grain surface (upper left) showing typical stage 2 alteration. Etching of the surface is visible, apparently leaching along preferred crystallographic directions. Clay aggregates grow nestled into the surface grooves. K-content suggests that the clay aggregates are probably illite, or K-smectite.

Figure 3 — Same as Figure 1. Bar scale = 1 μm. Close-up of one of the phyllosilicate aggregates seen in the top center part of SEM micrograph (Figure 2). Note how the clays appear to be an integral part of the K-feldspar crystal. The surface of the slightly etched feldspar seems to have a coating of an ultrathin, highly disordered or amorphous material, possibly allophane or iron oxides. At mid center the faint etching lineation constructs an angle of 120° with a sharp surface.

Figure 4 — Bar scale = 20 μm. Subhedral to subrounded pure K-feldspar grain showing stage 3 surface alteration. Overview of grain with phyllosilicate cover clinging to the surface.

Figure 5 — Same as Figure 1. Bar scale = 10 μm. Detail of center part of grain where clay mantle has cracked and separated due to ultrasonic treatment. Reveals feldspar face showing vague crystallographic orientation. Surface broken down into tiny step-like blocks.

Figure 6 — Same as Figure 4. Bar scale = 1 μm. Ultramorphology of contact between feldspar crystal surface (left) and monomineralic phyllosilicate coating (right). EDAX readings show Si, Al, K, and traces of Fe on crystal and Si (strong), K, Al, Fe, and a trace of Na(?), Mg. Mixed-layer illite/montmorillonite or K-smectite. Morphology is caused by an irregular aggregate of rolled and buckling sheaves with a poorly developed crystal habit.

PLATE 12

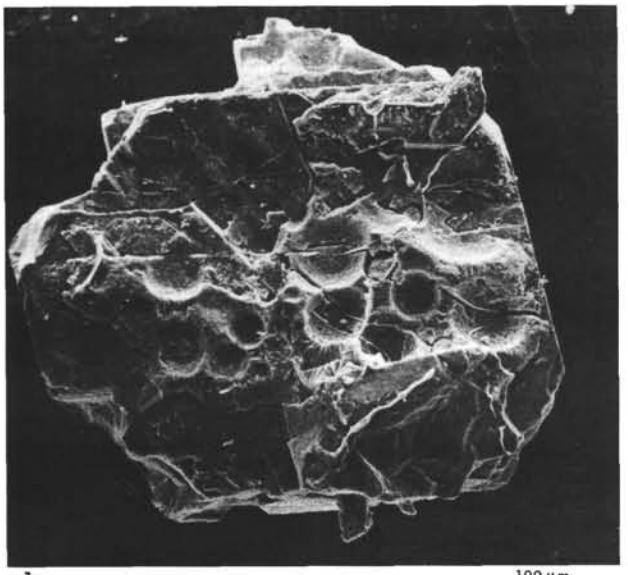

1

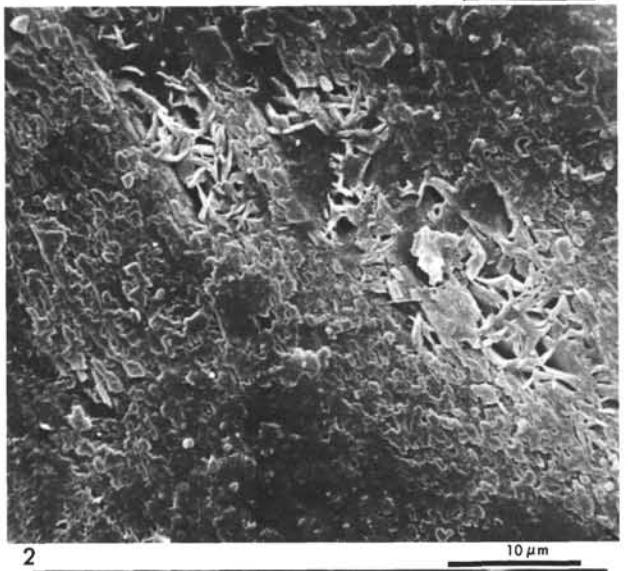

2

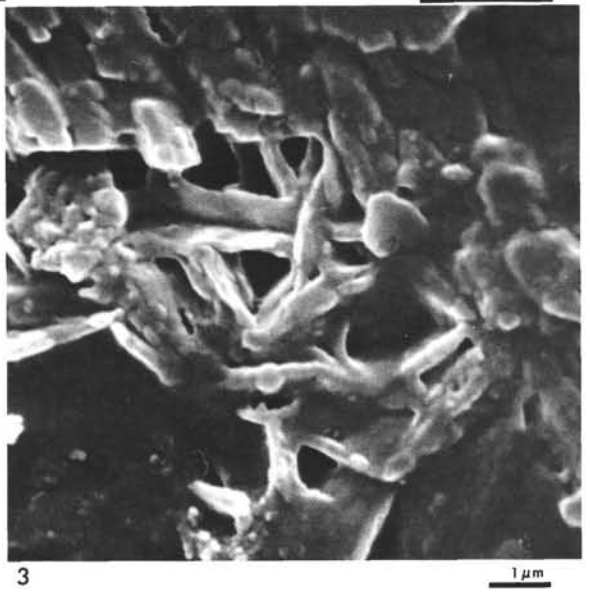

3

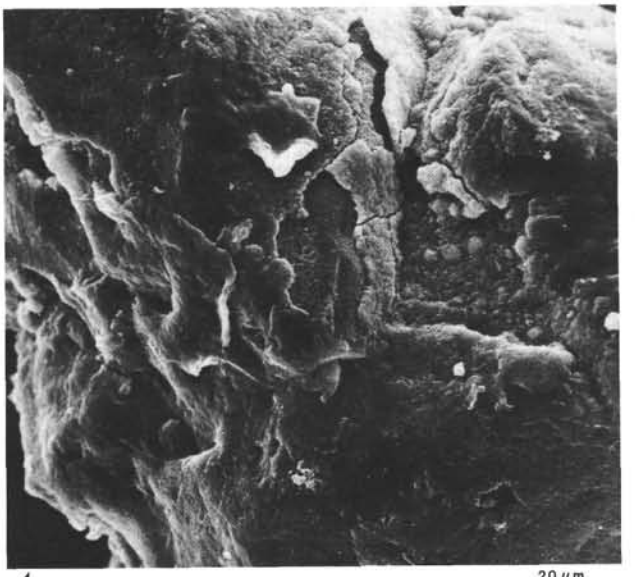

4

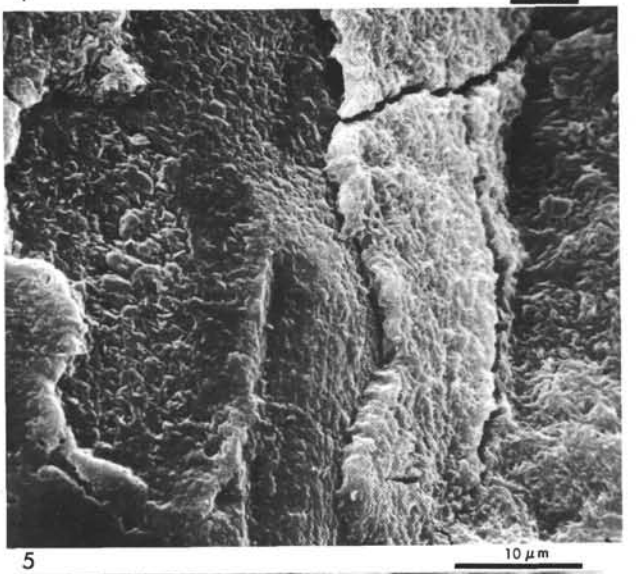

5

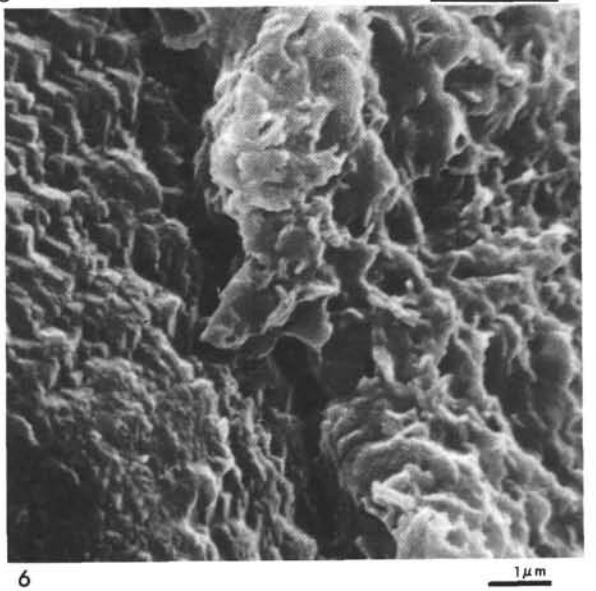

6

PLATE 13

Scanning electron micrographs of surface alteration morphologies on pure K-feldspar.

Figure 1 — 315A-29-2, 22-26 cm (970 m depth). Santonian(?). Bar scale = 50 μm. Overview of a translucent K-feldspar grain. A greenish mat of phyllosilicate minerals coats the surface, and an altered greenish glass is sandwiched between feldspar layers. The detail views (Figures 2 and 3) below are from the surface of the feldspar protrusion visible in the lower part of the picture.

Figure 2 — Same as Figure 1. Bar scale = 1 μm. Ultramorphology of a furrow in the feldspar grain. Skeletal bridges probably are a remnant of silicate framework. EDAX analysis of phyllosilicate mass visible in upper part of the micrograph displays Al (strong), Si, K, Fe from a probable mixed-layer assemblage. Note the platelets parallel to the crystal surface.

Figure 3 — Same as Figure 1. Bar scale = 1 μm. Authigenic mineral growth is from a phyllosilicate mass. EDAX analysis only registered Si and a trace of Fe suggesting that this is authigenic quartz growth from the alteration of the montmorillonite.

Figure 4 — 315A-30-2, 92-94 cm (990 m depth). Santonian(?). Bar scale = 100 μm. Overall view of a pitted K-feldspar grain. Maybe a highly altered anorthoclase grain. Optically the grain is homogeneous, milky white, with a matty surface, and shows rounding of the crystal faces. Note the presence of hollow structures on the surface and pits oriented along lattice planes.

Figure 5 — Same as Figure 4. Bar scale = 10 μm. Surface morphology of a moderately clean area on the upper right part of the grain. Note the intensive etching with preferred orientations. Dissolution seems to be undercutting the feldspar surface. EDAX measurements on a flat area in the center of the SEM confirmed the K-feldspar composition with Si, Al, and K as the only peak with a trace of Fe. Note the lack of clay crystals. The alteration is a variant of the stage 1 leaching.

Figure 6 — Same as Figure 4. Bar scale = 1 μm. Ultramorphology of the feldspar surface around one of the etch-pits. Note how the surface is coated with an ultra-thin layer)of tiny globules. The composition of this phase in unknown, but may represent an amorphous phase of silica, iron oxide, or allophane.

PLATE 13

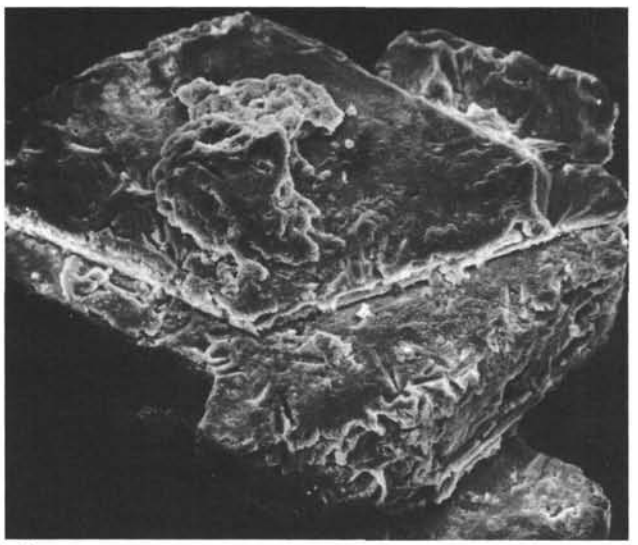

1

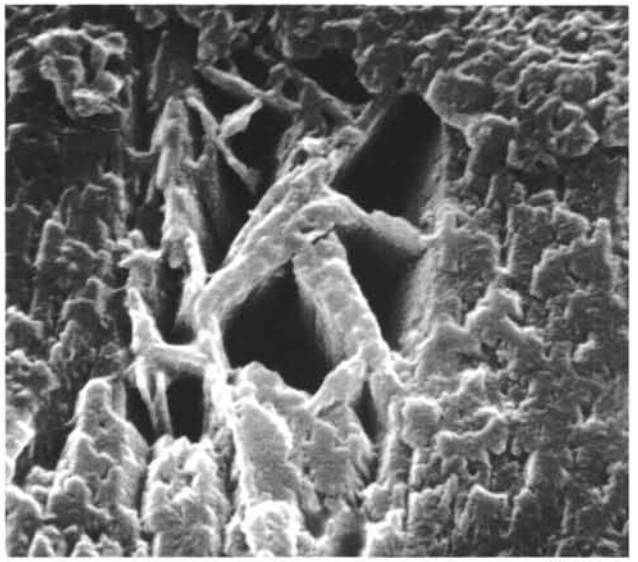

2

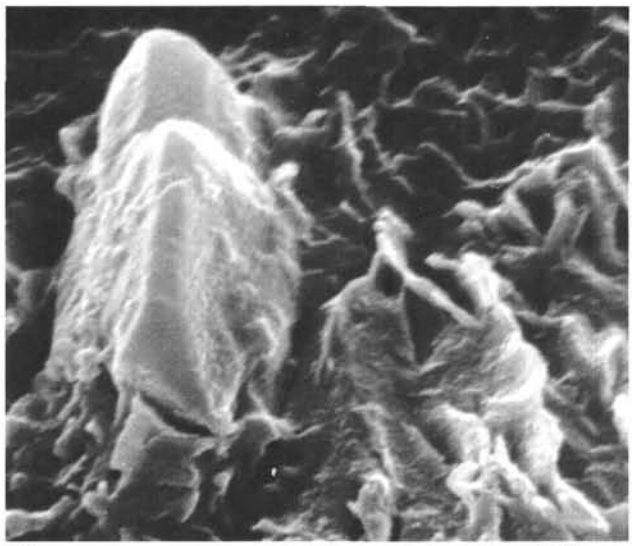

3

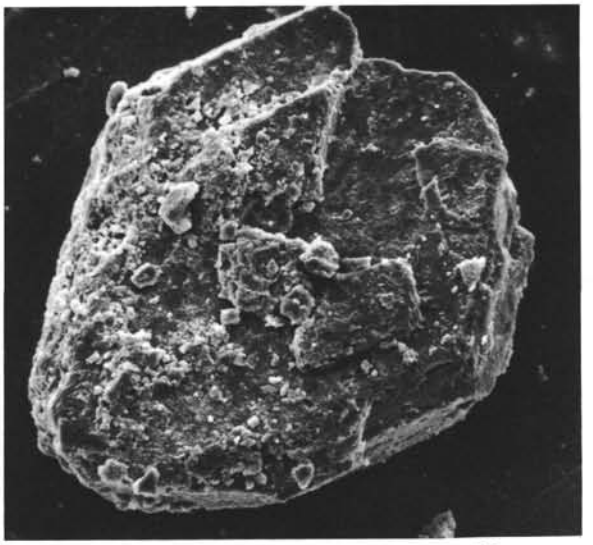

4

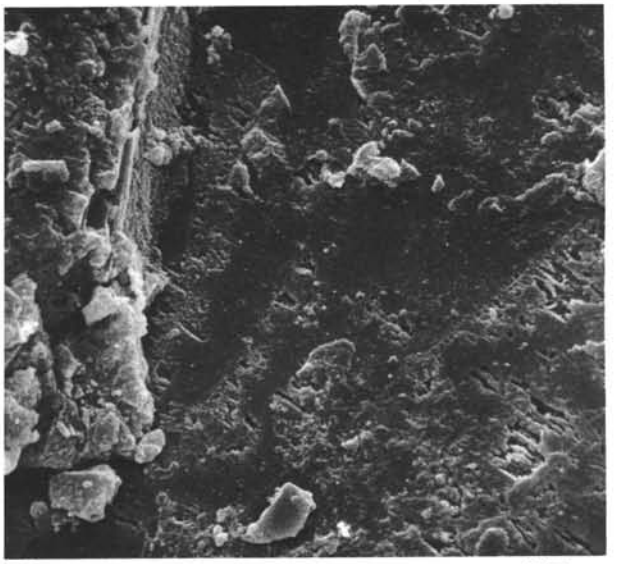

5

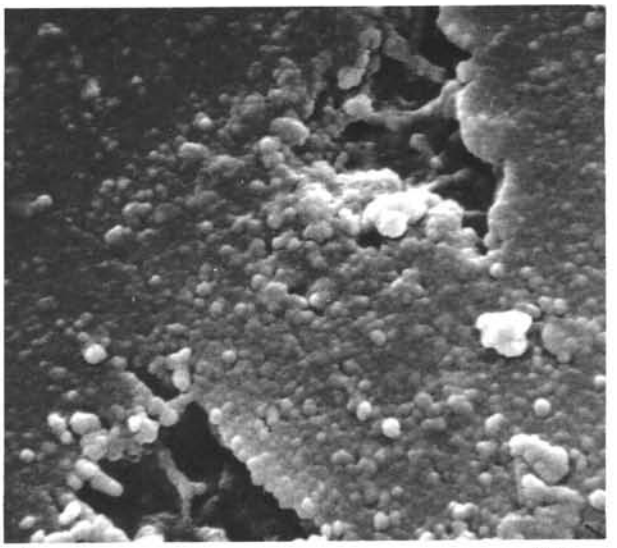

6

PLATE 14

Scanning electron micrographs comparisons of surface phyllosilicate volcanic grains. Sample 315-29-2, 22-26 cm (970 m depth). Santonian(?).

Figure 1 — Bar scale = 100 μm. Subhedral pyroxene grain is shown as a comparison with the previous feldspar grains. The grain surface is highly altered, exhibiting a thick mantle of clay minerals, most probably montmorillonites and/or chlorite. Crystallographic faces vaguely visible. EDAX analysis on fresh-looking edge (left) reveals composition of Si, Fe, Al, Mg, and traces of Ca and K, suggesting a clinopyroxene. The clay coating on the grain registers Fe, Si, Al, K which suggests an iron-rich K-smectite or mixed-layered clay.

Figure 2 — Same as Figure 1. Bar scale = 1 μm. Close-up of clay coating on the grain which has peeled off to reveal similar phyllosilicate layers below.

Figure 3 — Bar scale = 20 μm. Egg-shaped grain of greenish-black altered basaltic glass. Surface completely altered to a thick coating of clays with an EDAX composition containing Fe, Si, Al, Mg, and a trace of K, suggesting a chlorite or chlorite/montmorillonite or K-smectite phase. Note that the fracture in the grain surfaces reveals that alteration is mostly confined to the surface.

Figure 4 — Same as Figure 3. Bar scale = 1 μm. Ultramorphology of the surface coating. Similar to Figure 2 above. Note the globular or vermiform nature of the clay platelets and lack of well-developed crystal habit. May represent a mixed-layered assemblage.

Figure 5 — Bar scale = 10 μm. Pitted surface of a K-feldspar grain with phyllosilicate growth.

Figure 6 — Same as Figure 5. Bar scale = 1 μm. Newly formed clays with moderately well developed crystal form appear to lift-up from the surface as the feldspar surface is broken down. Morphology different than the phyllosilicates from Figures 2 and 4.

PLATE 14